Progress In Electromagnetics Research, PIER 10, 217–270, 1995

COUPLED-MODE THEORY FOR OPTICAL WAVEGUIDES

B. E. Little and W. P. Huang

1. Introduction

Coupled-mode theory (CMT) has had a lengthy and diverse development. It was initially introduced in the early 1950's for microwave devices, and latter applied to optical devices in the early 1970's. The theory's appeal was its usefulness in analyzing devices and predicting fundamental characteristics by simple analytic means, tractable to computational devices of the time. Today, as computer power has

increased almost exponentially, the usefulness of CMT has not diminished. Instead, it has become an integral part of the whole design process. This success has resulted from the theory's wide applicability, intuitive feel, and often surprising accuracy, especially when one considers the simplicity of the governing equations. It is perhaps one of a handful of 'synthesis' tools, since unlike numerical schemes which are 'analysis' by nature, the possibility always exists for inverting the coupling equations and solving for waveguide parameters given some desired response.

The essence of coupled-mode theory is clear; one treats the composite or compound waveguiding structure as a collection of simpler waveguides, with the modes associated with each individual (component) waveguide being perturbed by the presense of the others or any additional nonuniformity. These perturbations lead to coupling and exchange of power among the guided modes. Since we are ultimately interested in the manipulation of a particular guided mode, rather than the whole compound field, this coupling of modes formalism represents a rather appealing conceptual framework.

In its rigorous derivations, coupled-mode theory is a restatement of Maxwell's equations as long as all the boundary conditions can be satisfied, and is hence exact. However, it is always the case that only a finite number of expansion modes are used, and in this respect coupled-mode theory is an approximate approach. This compromise in rigorousness is well compensated for in a number of respects: (i) It is very intuitive and insightful. The theory interprets the device physics through coupling coefficients, which clearly show their dependency on the selection of device geometry. This leads to predictable and exploitable power transfer characteristics; (ii) It allows for quick feasibilities studies and the demonstration of possible new principles. It also gives a starting point to which other more rigorous methods (detailed in later chapters) would then be employed to fine tune parameters; (iii) Although not exact, the solution often tend to be quite accurate, and the accuracy sometimes improved by a better selection of known 'trial solutions'. Altogether, the theory can be said to 'pick-up' salient power transfer characteristics with a measure of reliability.

In the following sections the nonorthogonal coupled-mode theory (NCMT) is developed in a rigorous fashion as a general framework which is subsequently applied to various coupling scenarios. These include the parallel coupler (directional coupler), grating-assisted

coupling, and coupling induced by changes of the waveguide separation (tapering). As a separate issue, the need to account for the birefringence induced by an adjacent waveguide is discussed. In all cases the structures are assumed to be lossless and isotropic (with extensions to be highlighted), but otherwise of arbitrary transverse shape.

The goal in the following sections will be to establish a set of equations governing the evolution of an arbitrary number of modes, each which is coupled through various possible mechanisms. In matrix form, this will have the appearance

$$\mathbf{P}\frac{d}{dz}\mathbf{A} = -j\mathbf{H}\mathbf{A} - j\tilde{\mathbf{K}}\mathbf{A} - \mathbf{F}\mathbf{A}$$

where $\mathbf{A}$ represents a vector containing the amplitudes of the modes in the system, $\mathbf{P}$ is a power matrix, $\mathbf{H}$ is a matrix that governs self and evanescent coupling, $\tilde{\mathbf{K}}$ will represent coupling due to periodic grating perturbations, and $\mathbf{F}$ is due to taper induced coupling.

Before embarking on the analysis, the development of the coupled-mode theory is traced from its origins in microwave applications in the early 1950's, through its evolutionary paths, extensions and problems, and crediting the advancements made by the many contributors who have pioneered the development of the various formulations.

1.1 Historical Review.

The concept of mode coupling in electromagnetics was first developed by Pierce [1] in 1954 for applications involving traveling-wave tubes. In the same year Miller [2] introduced a coupled-mode theory for the description of microwave waveguides and passive devices. The theory was soon generalized by Louisell [3] to treat tapered waveguide structures, where the coupling coefficients depend on the propagation distance. The early formulations were developed on the basis of power conservation arguments and were rather heuristic. More rigorous formulations of the coupled-mode equations were later established by Schelkonof [4] using a mode expansion, and Haus [5] using a variational principle.

The coupled-mode theory for optical waveguides was developed by Snyder [6], Marcuse [7], Yariv [8], and Kogelnik[9] in the early 1970's. It has since been applied to a vast number of guided wave, optoelectronic, and optical fiber devices, such as, directional couplers made of thin film and channel waveguides[10–12], fiber couplers [13], distributed

feedback lasers [14], distributed Bragg reflectors [15], grating coupled waveguides [16], nonparallel structures [17], polarization rotation [18], and guide mode to radiation mode coupling [19]. It has also been extended to describe coupling induced by nonlinear material response such as, harmonic generation in waveguides [20], modulation instability [21] in fibers, and nonlinear couplers [22]. There are also several excellent reference books available on the subject [23–29].

The analysis of coupled-waveguide systems by the conventional orthogonal coupled-mode theory (OCMT) was based almost exclusively on the modes of the individual or uncoupled waveguides. Once these waveguide modes, i.e., their propagation constants and field patterns are determined, the amplitudes of the modes in the coupled-waveguide systems are governed by the coupled-mode equations. The solutions of the coupled-mode equations describe wave propagation and coupling in the coupled waveguide system. Together with the transverse field distribution, the coupled-mode analysis provides a simple, intuitive, yet rigorous description of the electromagnetic wave propagation and interaction in a coupled-waveguide system.

A number of approximations are assumed in the formulations and often the solutions of the coupled-mode equations. One of the assumptions in the conventional OCMT, is that the waveguide modes are orthogonal to each other. This approximation was considered to be acceptable and taken for granted until Hardy and Streifer [30] in 1986 suggested a modified coupled-mode formulation in which the nonorthogonality was considered. This new nonorthogonal coupled-mode theory was shown to yield more accurate dispersion curves and field patterns for the composite modes (or normal modes) of the parallel coupled waveguides. In their original paper, Hardy and Streifer did not establish the self-consistency of their formulations by demonstrating power conservation for a lossless system. A self-consistent nonorthogonal coupled-mode formulation for the parallel coupled-waveguide system was later developed by Haus and coworkers using a variational principle [31], by Chuang using the reciprocity theorem [32], and also by Hardy and Streifer through reformulation [33]. There were some minor discrepancies among the various formulations advanced by different groups [31–33]. These differences were examined by Vassello [34] and shown to be subtle theoretically, but of little practical significance.

In the course of the development, criticism was raised by Snyder and coworkers about the validity and accuracy of the new nonorthogo-

nal CMT. In a series of papers [35,36], they showed that the nonorthogonal formulations could lead to erroneous results for the coupling length of the TM modes of parallel slabs when the index discontinuity is large. The origin of the error is apparent in this case since the waveguide modes used as the trial solution in the coupled-mode theory are subject to significant error when the index steps are large. However, they also demonstrated that the conventional orthogonal coupled-mode theory based on the same waveguide modes more accurately predicted the coupling length for the case of large index differences. This finding was somewhat unexpected, and triggered a series of debates in the field [35-43]. It was later resolved by Haus, Huang and Snyder [44].

Despite the controversies, the nonorthogonal CMT attracted much attention and was applied to a range of optical guided-wave devices based on coupled-waveguide structures. Simplified scalar versions were advanced [45–50]. Formulations for multiwaveguide and/or multimode structures [51–55], anisotropic media [56–58], periodic grating structures [59–67], tapered structures [68–75] and nonlinear couplers [76] were developed. Applications to various directional couplers in integrated and fiber optics [77–82] were carried out. Some experimental work by Marcatili and coworkers [83], and Syms and coworkers [84] were also published and their findings appeared to support the merit of the nonorthogonal CMT.

2. The Parallel Directional Coupler

The directional coupler composed of two (or more) arbitrarily shaped, but otherwise uniformly parallel waveguides placed in close proximity, represents a fundamental component or building block of a large class of devices. Theoretically, the parallel coupler may be treated by two approaches, the normal-mode approach, or the coupled-mode theory. In the normal mode approach the exact modes of the compound structure are obtained. Since the normal modes do not exchange power over the length of the coupler, the situation is reduced to an interface problem: The input field excites a unique combination of normal modes at the input interface, these modes propagate uncoupled along the structure, and combine vectorially at the output interface, exciting the mode of the output waveguide in a unique fashion.

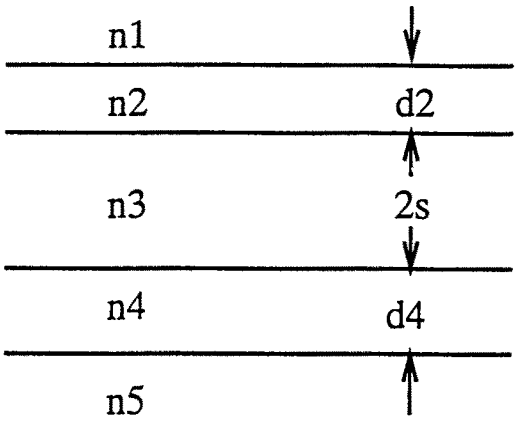

Figure 1. A schematic diagram of a uniform directional coupler.

Alternatively, the coupled-mode theory interprets the situation as a coupling between the component waveguide modes. This interpretation is intuitively advantageous, since the coupling mechanisms which gives rise to the different power and spectral characteristics are embodied explicitly in the coupling coefficients. A study of the coupling coefficients may thus lead to a deeper understanding of the factors leading to various device responses.

In this section the coupled-mode equations for the vector fields are rigorously formulated through a variational principle. The formulations are valid for linear and lossless waveguides of arbitrary cross sectional shape. The parallel slab coupler as shown in Fig. 1 will however, serve as our heuristic coupled mode device, since the exact modes are easily computed. For more complex waveguide shapes, one may calculate the mode profiles numerically, and employ the coupled-mode theory to analyze the coupling process along the coupler length.

2.1 A Variational Principle for the Propagation Constant.

Consider a lossless optical waveguide structure with an index that is a function of the transverse coordinates only. Maxwell's equations (with implied time dependence $e^{j\omega t}$) for the structure can be written as

$$\nabla_t \times \mathbf{E} + j\omega\mu_o \mathbf{H} = \lambda \hat{z} \times \mathbf{E}, \tag{1a}$$

$$\nabla_t \times \mathbf{H} - j\omega\epsilon \mathbf{E} = \lambda \hat{z} \times \mathbf{H}, \tag{1b}$$

where $\epsilon(x, y)$ is the dielectric constant of the medium and

$$\nabla_t = \hat{x}\frac{\partial}{\partial x} + \hat{y}\frac{\partial}{\partial y}. \tag{2}$$

Equations (1) may be generalized to anisotropic media by replacing the dielectric constant ϵ by a dielectric tensor. Multiply (1a) by $\mathbf{H}^*$, (1b) by $\mathbf{E}^*$, subtract and integrate the result over the entire cross section. Solving for λ one obtains [31]

$$\lambda = \int [\mathbf{H}^* \cdot (\nabla_t \times \mathbf{E} + j\omega\mu_o \mathbf{H}) - \mathbf{E}^* \cdot (\nabla_t \times \mathbf{H} - j\omega\epsilon \mathbf{E})] da$$

$$\times \left\{ \int [\mathbf{E} \times \mathbf{H}^* + \mathbf{E}^* \times \mathbf{H}] \cdot \hat{z} da \right\}^{-1} \tag{3}$$

Expression (3) can be shown to be stationary if both $\hat{\mathbf{n}} \times \mathbf{E}$ or $\hat{\mathbf{n}} \times \mathbf{H}$ are continuous, where $\hat{\mathbf{n}}$ is the unit normal vector to the boundaries across index discontinuities, and $\hat{\mathbf{n}} \times \mathbf{E}$ or $\hat{\mathbf{n}} \times \mathbf{H}$ vanish on an external boundary or at infinity.

2.2 Coupling of Modes Derived from the Variational Principle

The coupled mode equations will emerge from (3) when one substitutes for $\mathbf{E}$ and $\mathbf{H}$ a suitable set of trial solutions. The trial solution typically used is the superposition of the modes of the component waveguides

$$\mathbf{E} = \sum_{i=1}^{N} a_i(z)\mathbf{e}_i(x, y), \tag{4a}$$

$$\mathbf{H} = \sum_{i=1}^{N} a_i(z)\mathbf{h}_i(x, y), \tag{4b}$$

where a_i are the modal amplitudes and $\mathbf{e}_i$ and $\mathbf{h}_i$ are the total electric and magnetic fields of the i th individual guide satisfying the following equations,

$$\nabla_t \times \mathbf{e}_i + j\omega\mu_o \mathbf{h}_i = j\beta_i \hat{\mathbf{z}} \times \mathbf{e}_i, \tag{5a}$$

$$\nabla_t \times \mathbf{h}_i - j\omega\epsilon_i \mathbf{e}_i = j\beta_i \hat{\mathbf{z}} \times \mathbf{h}_i. \tag{5b}$$

Here, $\epsilon_i = n_i^2$ is the dielectric constant distribution that defines the profile of the i th waveguide. If the waveguides are weakly guiding, the scalar modes may be used as the trial solutions [45–50].

At this point there may a be number of arbitrary ways in which the compound structure is decomposed into the component waveguides. For example, Fig. 2 shows two choices for the ϵ_i distributions of a two guide coupler. For practical considerations, one would chose the distribution that reproduces the input and output waveguides to the coupler.

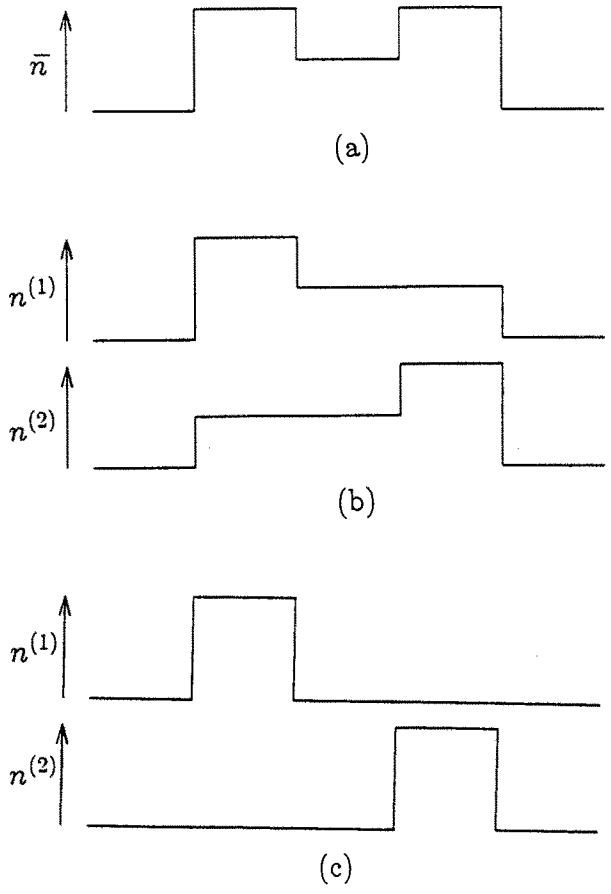

Figure 2. Index profile for a uniform slab coupler $\bar{n}$ in (a), with two choices for the individual waveguide profiles $n^{(i)}$ in (b) and (c).

By substituting (5) into the variational expression (3), one obtains for the system propagation constant

$$\lambda \equiv j\beta = j\frac{\sum_j a_i^* H_{ij} a_j}{\sum_j a_i^* P_{ij} a_j}, \tag{6}$$

where

$$H_{ij} = P_{ij}\beta_j + \kappa_{ij}, \tag{7}$$

$$P_{ij} = \frac{1}{4}\int (\mathbf{e}_i^* \times \mathbf{h}_j + \mathbf{e}_j \times \mathbf{h}_i^*) \cdot \hat{z} da, \tag{8}$$

$$\kappa_{ij} = \frac{1}{4}\omega\epsilon_o \int (\bar{n}^2 - n_j^2)\mathbf{e}_i^* \cdot \mathbf{e}_j da. \tag{9}$$

The optimum value of β under the assumed trial solution is obtained by extremimizing (6) by differentiating with respect to a_i^* or a_j,

$$j\beta \sum_j P_{ij} a_j = j \sum_j H_{ij} a_j. \tag{10}$$

The coupled mode equations result when one associates $-j\beta$ with the derivative of an assumed spatial dependence $e^{-j\beta z}$. With this replacement (10) becomes

$$\sum_j P_{ij} \frac{da_j}{dz} = -j \sum_j H_{ij} a_j \tag{11a},$$

or in matrix form

$$\mathbf{P}\frac{d}{dz}\mathbf{A} = -j\mathbf{H}\mathbf{A}. \tag{11b}$$

$\mathbf{P}$ is seen to be the power matrix associated with the waveguide modes, with the off-diagonal terms representing the cross-power arising from mode nonorthogonality. The matrix $\mathbf{H}$ is the overall (Hermitian) coupling matrix, with the terms κ_{ij} representing the evanescent or tunnel coupling due to the proximity of adjacent waveguides. The preceding derivation indicates that the coupled-mode equations result from an optimization by applying the variational principle. In this sense, the solutions to the equations represent the best possible solutions to the coupled waveguide system based on the trial solutions used. In the

above derivation, the system of waveguides are assumed to be lossless. A similar approach may be applied to lossy waveguides with some modifications to the cross-power and coupling coefficients [32].

For a lossless system, power conservation implies (see (44))

$$\frac{d}{dz}\sum a_i^* P_{ij} a_j = 0. \tag{12}$$

It follows from (11) that

$$H_{ij} = H_{ji}^*, \tag{13a}$$

or

$$P_{ij}(\beta_j - \beta_i) = \kappa_{ij} - \kappa_{ji}^*. \tag{13b}$$

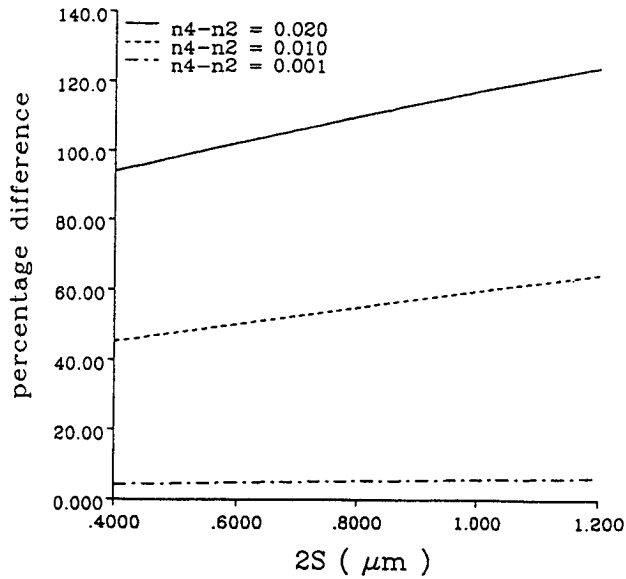

Figure 3. The percentage difference between the normalized coupling coefficients: $2(\kappa_{12}-\kappa_{21})/(\kappa_{12}+\kappa_{21})$, as a function of the guide separation for TE modes of an asymmetric slab coupler. $n_1 = n_3 = n_5 = 3.20$ and $n_2 = 3.25$. The index n_4 varies as $\delta n = n_2 - n_4 = 0.01, 0.1, 0.2$. The widths of the two slabs are $d_2 = d_4 = 1.0\mu m$. The wavelength is $\lambda = 1.5\mu m$.

We note that, unless $\beta_i = \beta_j$, κ_{ij} is not equal to κ_{ji}^*. This is in contrast with the conventional orthogonal coupled-mode formulation which states that the coupling coefficients are symmetrical for a loss free system, regardless of the difference between the β_i's. Figure 3

shows $(\kappa_{12} - \kappa_{21})/\bar{\kappa}$ in percentage as a function of the separation $2S$ between the two slab waveguides of Fig. 1. The parameter $\bar{\kappa}$ is the average of the two coupling coefficients, i.e., $\bar{\kappa} = (\kappa_{12} + \kappa_{21})/2$. The indices of the waveguides are $n_1 = n_3 = n_5 = 3.20$ and $n_2 = 3.25$. The index of the other guiding layer is varied as $\delta n = n_4 - n_2 = 0.01, 0.1, 0.2$, respectively. The widths of the two slabs are $d_2 = d_4 = 1.0\mu m$. The wavelength is $\lambda = 1.5\mu m$. The results indicate that κ_{12} is nearly equal to κ_{21} when the two waveguides are very similar. However, the percentage difference between κ_{12} and κ_{21} can be as large as 100% as the degree of the asymmetry increases. We also note that the percentage difference does not vanish as the distance separating the two waveguides become large. In this sense, there is an inherent inconsistency in the conventional coupled-mode theory based on the individual waveguide modes when it is applied to couplers made of dissimilar waveguides. This fact was first pointed out by Hardy and Streifer [30] and subsequently demonstrated by others [31,32].

2.3 Transformations for the Two-Guide Coupler

We will now restrict our attention to forward propagating modes. In the two guide coupler, we assume power normalization of the fields to be $P_{11} = P_{22} = 1$ and let the cross-powers $P_{12} = P_{21} = X$. (For two-mode contradirectional coupling, we would find $P_{11} = 1$, $P_{22} = -1$, and $X = 0$, i.e., orthogonality of the modes whether the modes belong to the same waveguide of not.) The power matrix has the form

$$\mathbf{P} = \begin{pmatrix} 1 & X \\ X & 1 \end{pmatrix}, \tag{14}$$

while the coupling matrix $\mathbf{H}$ may be written as

$$\mathbf{H} = \begin{pmatrix} \beta_1' & \kappa \\ \kappa & \beta_2' \end{pmatrix}, \tag{15}$$

where

$$\begin{aligned} \beta_1' &= \beta_1 + \kappa_{11} \\ \beta_2' &= \beta_2 + \kappa_{22} \\ \kappa &= X\beta_1 + \kappa_{21} \\ &= X\beta_2 + \kappa_{12}. \end{aligned} \tag{16}$$

The β_i' are the perturbed propagation constants, while κ is the effective evanescent coupling.

Although it is possible to solve (11b) by rewriting it as [30]

$$\frac{d}{dz}\mathbf{A} = -j\mathbf{P}^{-1}\mathbf{H}\mathbf{A}, \tag{17}$$

through multiplication of the inverted power matrix, we will find it more expedient to apply an orthogonalizing transformation, followed by a diagonalizing transformation. These transformations will be shown to yield the (approximate) normal modes of the compound structure.

2.4 Orthogonalization

The power matrix $\mathbf{P}$ is positive definate, thus it can be written as a product of a matrix and its adjoint

$$\mathbf{P} = \mathbf{Q}^{+}\mathbf{Q}, \tag{18}$$

where the superscript '+' is the adjoint operator and $\mathbf{Q}$ is expressed as

$$\mathbf{Q} = \begin{pmatrix} \cos\frac{\alpha}{2} & \sin\frac{\alpha}{2} \\ \sin\frac{\alpha}{2} & \cos\frac{\alpha}{2} \end{pmatrix}, \tag{19}$$

with $X = \sin\alpha$. By using (18) in (11b) and multiplying through by $(\mathbf{Q}^{+})^{-1}$, a new set of power-orthogonal modes labeled $\mathbf{B}$ are defined

$$\mathbf{B} = \mathbf{Q}\mathbf{A}. \tag{20}$$

The $\mathbf{B}$ modes are seen to be power orthogonal, since the total power is shown to be (section 2.6), $\mathbf{B}\mathbf{B}^{*} = \mathbf{A}^{t}\mathbf{P}\mathbf{A}^{*}$, that is, equal to the sum of the squares of the individual modal amplitudes. The coupled-mode equations are reduced to

$$\frac{d}{dz}\mathbf{B} = -j\mathbf{H}'\mathbf{B}, \tag{21}$$

where the new coupling matrix $\mathbf{H}'$ remains Hermitian, and is defined through

$$\mathbf{H}' = [\mathbf{Q}^{+}]^{-1}\mathbf{H}\mathbf{Q}^{-1}. \tag{22}$$

Notationally, we express $\mathbf{H}'$ as

$$\mathbf{H}' = \begin{pmatrix} c_{11} & c_{12} \\ c_{21} & c_{22} \end{pmatrix}, \tag{23}$$

where

$$\begin{aligned} c_{11} &= \frac{\bar{\beta}-X\kappa}{1-X^2} + \frac{\Delta}{\sqrt{1-X^2}} \\ c_{22} &= \frac{\bar{\beta}-X\kappa}{1-X^2} - \frac{\Delta}{\sqrt{1-X^2}} \\ c_{12} &= \frac{\kappa-X\bar{\beta}}{1-X^2} = c_{21} = \frac{\kappa_{12}+\kappa_{21}-X(\kappa_{11}+\kappa_{22})}{2(1-X^2)} \end{aligned} \tag{24}$$

and

$$\bar{\beta} = \frac{\beta_1' + \beta_2'}{2}, \tag{25a}$$

$$\Delta = \frac{\beta_1' - \beta_2'}{2}. \tag{25b}$$

Here, $\bar{\beta}$ is the average propagation constant, while Δ is the degree of asynchronisity between the coupled guides. For maximum power transfer, the condition $\Delta = 0$ is required.

Of special note in the above transformations is the effect of neglecting the nonorthogonality of the modes, that is, neglecting X. Then, $\mathbf{P} = \mathbf{Q} = \mathbf{I}$, (unit matrix), and the $\mathbf{B}$ modes reduce to the waveguide modes ($\mathbf{A}$ modes), with one important difference. By rewriting c_{12} and c_{21} as the final right hand expression in (24), it is seen that the coupling terms are symmetrized by taking the average of κ_{12} and κ_{21}. Now the orthogonal coupled-mode theory (i.e., $X \to 0$) for the waveguide modes becomes self-consistent, i.e., power is conserved when $\kappa_{12} \neq \kappa_{21}$. The power-orthogonal mode formulation presently derived will also be found useful in analyzing tapered couplers in section (4).

2.5 Diagonalization

By diagonalizing $\mathbf{H}'$ through a unitary transformation, a new set of modes are defined, which are decoupled. These are the equivalent normal modes of the compound structure. Introduce the unitary transformation by

$$\mathbf{B} = \mathbf{UW}, \tag{26}$$

where

$$\mathbf{U}^{+}\mathbf{U} = \mathbf{I}. \tag{27}$$

The resulting coupled equations describing the interactions of $\mathbf{W}$ are

$$\frac{d}{dz}\mathbf{W} = -j[\beta_{s,a}]\mathbf{W}, \tag{28}$$

with

$$\mathbf{U}^{+}\mathbf{H}'\mathbf{U} = [\beta_{s,a}], \tag{29}$$

and where $[\beta_{s,a}]$ is a diagonal matrix with elements β_s and β_a. There is no coupling between the two modes in (28). Hence, $\mathbf{W}$ may be interpreted as the amplitude vector for the normal modes of the parallel waveguides with propagation constants β_s and β_a, representing the even (symmetric), and odd (antisymmetric), compound modes respectively. These propagation constants are evaluated as

$$\beta_{s,a} = \frac{\bar{\beta} - X\kappa}{1 - X^2} \pm \sqrt{\frac{1}{1 - X^2}(X\bar{\beta} - \kappa)^2 + \frac{\Delta^2}{1 - X^2}}. \tag{30}$$

The unitary matrix is determined by requiring it to satisfy (29)

$$\mathbf{U} = \begin{pmatrix} \cos\frac{\phi}{2} & -\sin\frac{\phi}{2} \\ \sin\frac{\phi}{2} & \cos\frac{\phi}{2} \end{pmatrix}, \tag{31}$$

with

$$\tan(\phi) = \frac{2c_{12}}{c_{11} - c_{22}}, \tag{32}$$

and the c_{ij} are defined in (24). Equivalently

$$\phi = \tan^{-1}\{\frac{\kappa_{12} + \kappa_{21} - X(\kappa_{11} + \kappa_{22})}{\beta_1 - \beta_2 + \kappa_{11} - \kappa_{22}}\sqrt{1 - X^2}\}. \tag{33}$$

One may proceed directly from the waveguide mode formulation to the normal modes through the transformation

$$\mathbf{A} = \mathbf{O}\mathbf{W}. \tag{34}$$

From the orthogonalization and diagonalization procedures

$$\mathbf{O} = \mathbf{Q}^{-1}\mathbf{U}, \tag{35}$$

with (27) and (29) recast into

$$\mathbf{O}^{+}\mathbf{P}\mathbf{O} = \mathbf{I}, \tag{36}$$

$$\mathbf{O}^{+}\mathbf{H}\mathbf{O} = [\beta_{s,a}]. \tag{37}$$

The direct transformation matrix $\mathbf{O}$ then has the components

$$\mathbf{O} = \frac{1}{\cos\alpha}\begin{pmatrix} \cos\frac{(\phi+\alpha)}{2} & -\sin\frac{(\phi+\alpha)}{2} \\ \sin\frac{(\phi-\alpha)}{2} & \cos\frac{(\phi-\alpha)}{2} \end{pmatrix}. \tag{38}$$

The modes defined by $\mathbf{W}$ are approximations to the exact normal modes of the structure. The propagation constants of these normal modes are approximated by (30), while the field patterns are simply determined through (4) or inversion of (34). Equation (28) for the normal modes can be readily integrated analytically, and the transfer of power is discussed in the following section. The field patterns of the symmetric normal mode $\mathbf{e}_s$, and the antisymmetric normal mode $\mathbf{e}_a$, generated by (34) are respectively

$$\mathbf{e}_s = \frac{\cos\left(\frac{\eta+\alpha}{2}\right)}{\cos(\alpha)}\mathbf{e}_1 + \frac{\sin\left(\frac{\eta-\alpha}{2}\right)}{\cos(\alpha)}\mathbf{e}_2, \tag{39a}$$

$$\mathbf{e}_a = -\frac{\sin\left(\frac{\eta+\alpha}{2}\right)}{\cos(\alpha)}\mathbf{e}_1 + \frac{\cos\left(\frac{\eta-\alpha}{2}\right)}{\cos(\alpha)}\mathbf{e}_2. \tag{39b}$$

Note that due to the nonothogonality, a coupler composed of two identical waveguides does not have normal modes which have equal excitation from $\mathbf{e}_1$ or $\mathbf{e}_2$.

To assess the accuracy of the coupled-mode formulations established above, we calculated both the propagation constants and the field patterns of the composite modes of a parallel directional coupler. The parameters are the same as those used in Fig. 3, except that the refractive index n_4 is chosen to be 3.25 and 3.23 for a symmetric and a nonsymmetric case, respectively. Figures 4a and 4b show the effective indices of the TE composite modes as a function of waveguide separation. It is demonstrated that the nonorthogonal CMT (dash) yieids dispersion curves in closer agreement with the exact solutions (solid) than the self-consistent orthogonal CMT (dash-dot), in particular when the two waveguides are closely coupled. The electric field patterns for

the composite modes are shown in Fig. 5 and Fig. 6 for the cases of Fig. 4a and Fig. 4b respectively. The two selected separations between the slabs in each case are $2S = 1.0$ and $0.2\mu m$, representing a weak and a strong coupled waveguide system, respectively. In comparison with the exact solutions (solid), the nonorthogonal CMT (dash) is indeed superior to the orthogonal CMT (dot) for the field patterns. As a matter of interest, we also plotted the field patterns of the waveguide modes (dash-dot). The waveguide modes become acceptable approximations to the exact composite modes only when the two waveguides are weakly coupled and far from synchronism.

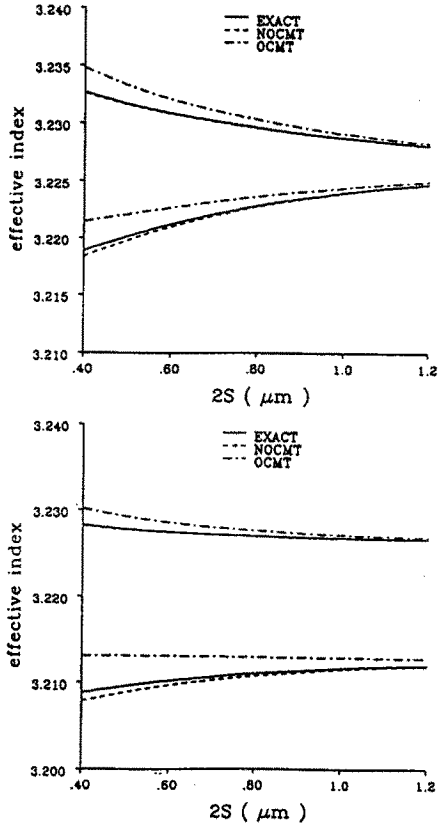

Figure 4. The effective indices of the symmetric- and the antisymmetric-like composite modes of two uniform directional couplers as a function of guide separation. (a) identical waveguides; (b) dissimilar waveguides. Solid: exact; dash: nonorthogonal CMT; dash-dot: orthogonal CMT. The parameters are the same as those in Figure 3 except that $n_4 = 3.25$ in (a) and 3.23 in (b).

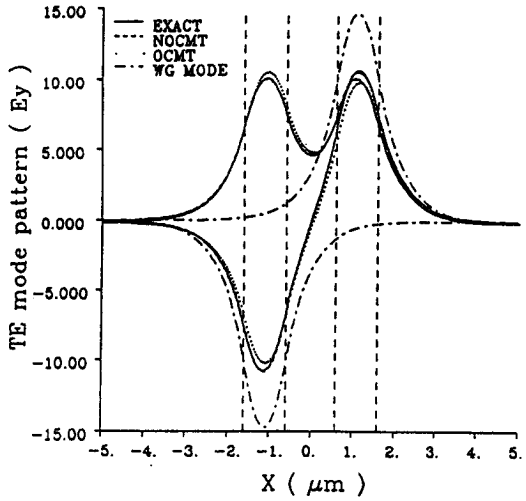

(a)

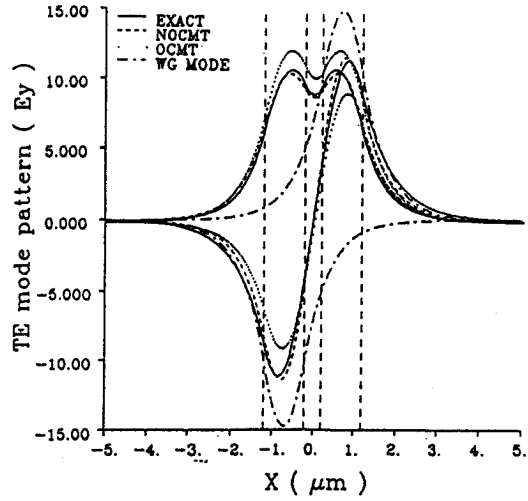

(b)

Figure 5. The electric field patterns of the symmetric- and the antisymmetric-like composite modes of the uniform directional couplers made of identical waveguides in Figure 4a. Solid: exact; dash: nonorthogonal CMT; dot: orthogonal CMT; dash-dot: waveguide modes. (a) $2S = 1.0\mu m$; (b) $2S = 0.2\mu m$.

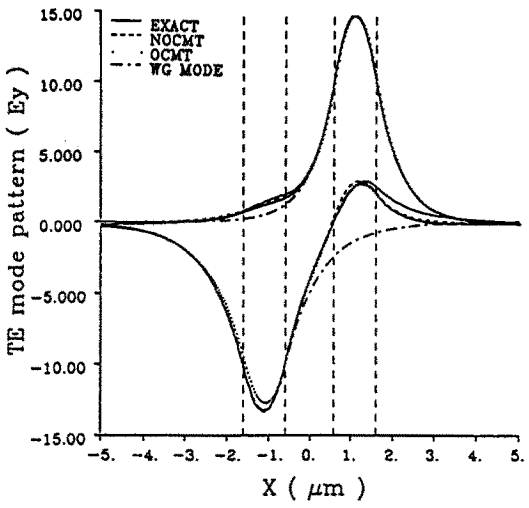

(a)

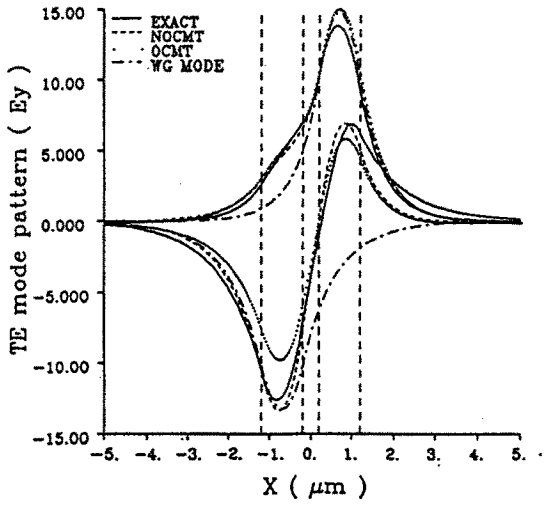

(b)

Figure 6. The electric field patterns of the symmetric- and the antisymmetric-like composite modes of the uniform directional couplers made of dissimilar waveguides in Figure 4b. Solid: exact; dash: nonorthogonal CMT; dot: orthogonal CMT; dash-dot: waveguide modes. (a) $2S = 1.0\mu m$; (b) $2S = 0.2\mu m$.

2.6 Power Flow between Waveguides

We now concentrate on the expressions for the flow of power from one waveguide to another, and on interpreting the power associated with one waveguide in a coupled system. Note that the normal modes (**W** modes) in (28) are decoupled, and hence immediately integrable. Applying the transformation (34), the resulting solution governing the evolution of waveguide amplitudes is

$$\mathbf{A}(z) = \mathbf{T}(z)\mathbf{A}(0), \tag{40}$$

where the transfer matrix $\mathbf{T}(z)$ is

$$\mathbf{T} = \mathbf{O}\begin{pmatrix} e^{-j\beta_s z} & 0 \\ 0 & e^{-j\beta_a z} \end{pmatrix}\mathbf{O}^{-1}, \tag{41}$$

or explicitly

$$t_{11} = t_{22}^* = \frac{\cos(\alpha)\cos(Sz) + j\cos(\eta)\sin(Sz)}{\cos(\alpha)}, \tag{42a}$$

$$t_{12} = j\frac{\sin(\eta + \alpha)\sin(Sz)}{\cos(\alpha)}, \tag{42b}$$

$$t_{21} = j\frac{\sin(\eta - \alpha)\sin(Sz)}{\cos(\alpha)}. \tag{42c}$$

The quantity S is one half the difference in the normal mode propagation constants, i.e., $S = (\beta_s - \beta_a)/2$. It will become clear shortly that S determines the coupling length L_c, through

$$L_c = \frac{\pi}{2S} = \frac{\pi}{\beta_s - \beta_a}, \tag{43}$$

where the coupling length (beat length) is defined as the distance over which the maximum amount of power is transferred from one waveguide to another.

The modal waveguide amplitudes at any point along the coupler are determined from (40). However, the power associated with a particular waveguide in a closely coupled array requires a revised definition.

For instance, the total power guided in the entire compound structure is defined in the usual sense by the Poynting theorem

$$P(z) = \frac{1}{4}\int (\mathbf{E} \times \mathbf{H}^* + \mathbf{E}^* \times \mathbf{H}) \cdot \hat{z} da$$

$$= \sum_{ij} a_i^*(z) P_{ij} a_j(z). \tag{44}$$

Due to the nonorthogonality, the total guided power is not only related to the magnitudes of the mode amplitudes $|a_i(z)|^2$, but also to the cross-product of different mode amplitudes through the overlap integrals (the cross-power terms).

To define the power associated with a particular guide, we envision the scenario in which that power would be measured. To do this one should terminate all the other guides so that the power may be guided out through only one of the guides as in Fig. 7. (There is no reflection at this termination since it is only 'virtual' in the sense of a definition for the modal power.) At z^-, the point just prior to the output position, the total fields may be expressed as a linear combination of the guided modes of the individual waveguides as in (4),

$$\mathbf{E} = \sum_j a_i \mathbf{e}_i(x, y), \tag{45a}$$

$$\mathbf{H} = \sum_j a_i \mathbf{h}_i(x, y). \tag{45b}$$

The fields at z^+, right after the termination, are expanded in terms of a superposition of the modes of the unterminated i^{th} waveguide

$$\mathbf{E} = b_i e_i(x, y) + \mathbf{E}_r, \tag{46a}$$

$$\mathbf{H} = b_i h_i(x, y) + \mathbf{E}_r, \tag{46b}$$

where $\mathbf{E}_r$ and $\mathbf{H}_r$ are the expansions in terms of radiation modes which, together with the guided mode, form an orthogonal and complete set. By mode matching at the junction, and using the orthogonality relations, the power in the output guide becomes

$$P_i(z) = |b_i(z)|^2 = \sum_j a_i^* P_{ij} a_j. \tag{47}$$

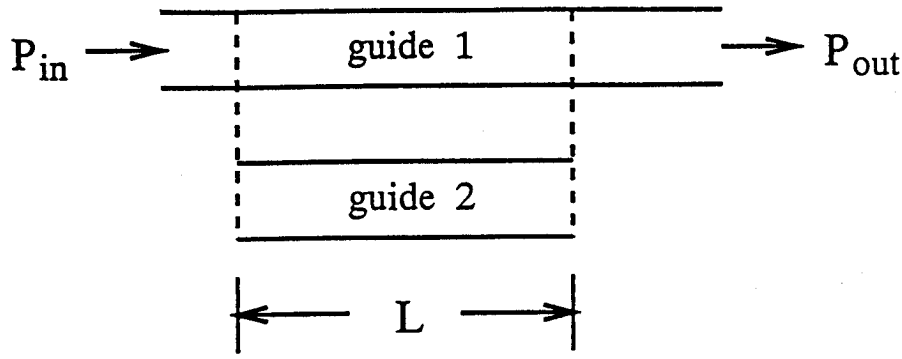

(a)

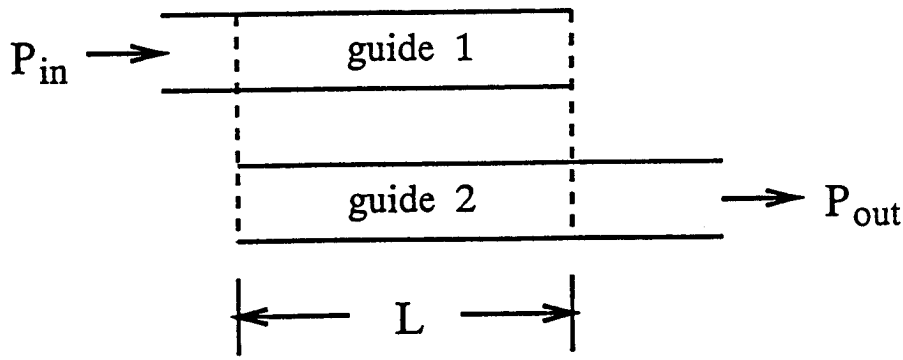

(b)

Figure 7. The input and output structures assumed for the guided power in an individual waveguide. (a) Guided power in waveguide 1; (b) Guided power in waveguide 2.

Note that due to the nonorthogonality between the modes, the fields in the other guides also contribute to the power in guide i. This is a source of cross-talk in optical switches [85,86]. For a two guide coupler, the definitions of power reduce to

$$P_i(z) = |a_i(z) + X a_j(z)|^2, \qquad (j \neq i). \tag{48}$$

Suppose that only guide 1 in initially excited, i.e., $a_1(0) = 1$, $a_2(0) = 0$. The powers determined from the transfer matrix and (48) are

$$P_1(z) = \cos^2(Sz) + \left[\frac{\cos(\phi) - \sin(\alpha)\sin(\alpha+\phi)}{\cos(\alpha)}\right]^2 \sin^2(Sz), \tag{49a}$$

$$P_2(z) = \sin^2(\alpha)\cos^2(Sz) + \sin^2(\phi)\sin^2(Sz). \tag{49b}$$

At one coupling length, $z = L_c = \pi/2S$, and for a perfectly phase-matched coupler ($\Delta = 0$ or $\phi = \pi/2$), the resulting power distribution is

$$P_1(L_c) = X^2, \tag{50a}$$

$$P_2(L_c) = 1. \tag{50b}$$

Therefore, after one coupling length complete power is transferred to guide 2. However, if the power in guide 1 is measured, we find that a portion of power, X^2, is still associated with guide 1 (due to the evanescent tail of mode 2). This does not violate power conservation. A rigorous normal mode analysis leads essentially to the same result [85].

Figures 8a and 8b show the coupling lengths as functions of separation for the two waveguide structures examined in Figs. 5 and 6. It is observed in Fig. 8a that the coupling length of the identical waveguides predicted by the nonorthogonal CMT (dash) is in excellent agreement with that produced by the self-consistent orthogonal CMT. This is understood by noting that the coupling length is related to the difference between β_s and β_a (or S). The coupling length is therefore not affected by the cross-power X as much as the individual propagation constants as was shown in Fig. 4a. Hence, when the two waveguides are similar and not too closely coupled, the simple conventional CMT gives an excellent approximation for the power transfer length. On the other hand, it is noted in Fig. 8b that the accuracy of the coupling length

predicted by the orthogonal CMT decreases as the two waveguides become dissimilar. At the same time, a similar but smaller decrease in accuracy of the nonorthogonal CMT is also observed.

(a)

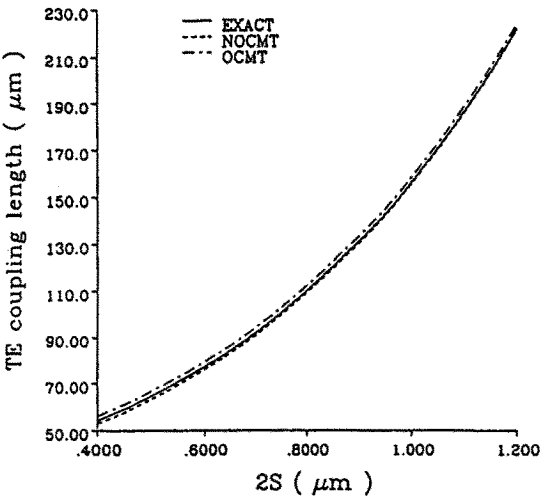

(b)

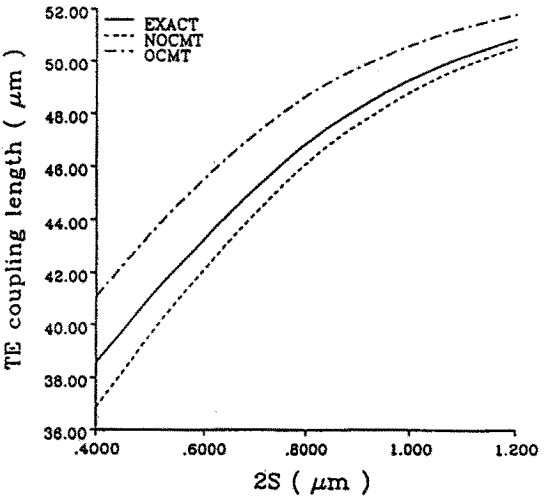

Figure 8. The coupling lengths as a function of guide separation for the TE modes of a slab coupler. Solid: exact; dash: nonorthogonal CMT; dash-dot: orthogonal CMT. (a) identical waveguides as in Figure 5; (b) dissimilar waveguides as in Figure 6.

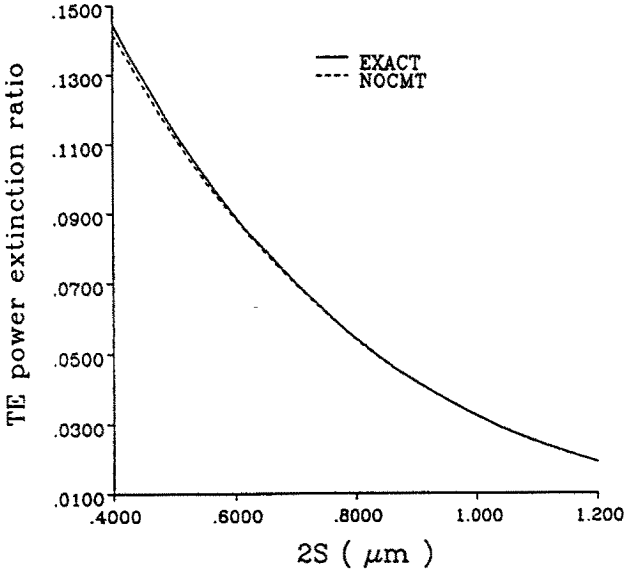

Figure 9. The power extinction ratio, or cross talk, as functions of separation for the TE modes of a symmetric slab coupler. Solid: exact; dash: NCMT. The parameters are the same as those in Figure 5.

The extinction ratio or cross-talk for the symmetric coupler in Fig. 8a is plotted in Fig. 9, using the results of (50a). We have also plotted the extinction ratio from the exact normal mode calculation [85,86], and it is seen that the two results agree very closely. The orthogonal CMT does not predict cross-talk for any separation.

3. Codirectional Grating Couplers

One of the most versatile of optical elements is the periodic grating. The grating acts as a mechanism in which to facilitate various forms of interaction between incident waves. These interactions may consist of two or more different optical beams, modes, frequencies or directions. In the field of integrated optics, the grating finds application in devices such as filters, couplers, mode converters, distributed

feedback oscillators and lasers, lens, and demultiplexers, to name a few. Nonlinear processes have also made extensive use of the grating, such as in parametric processes [87] and pulse compression [88]. The versatility of the grating is further enhanced if the grating period and/or grating strength is allowed to become a function of longitudinal distance (i.e., aperiodic or chirped). The fundamental principles of the grating have been studied rigorously and reviewed by Elachi [89], Gaylord and Moharam [90], and Yariv and Nakamura [91]. Typically, if the coupling caused within each individual grating period is small, then the uniform modes are not much affected, and coupled mode theory can yield reliable results.

Coupling between two integrated optical waveguides by means of a grating perturbation was first studied by Elachi and Yeh [92] in 1973 for forward coupling, and then in turn for backward coupling [93]. R. A. Syms [94] considered both the co- and contra-directional coupling interactions together to form a four port device. The study of the grating coupler was reiterated by Marcuse [95] by considering the coupling of array or compound modes, as opposed to the previous studies utilizing the isolated waveguide modes. Due to congruent developments in the uniform coupled-mode formulations at the time, the theory concerning grating-assisted codirectional coupling experienced many 'improved' reformulations [96–99]. The differences amongst these various reformulations attest to the fact that the overall behavior of the coupler is sometimes unclear, especially in the case of closely coupled waveguides.

3.1 General Principles

We consider here gratings that couple copropagating and collinear guided modes. In this case the periodicity of the perturbation is in the propagation direction, $\Delta n^2(x, y, z) = \Delta n^2(x, y, z + \Lambda)$, where Λ is the period. Our task in the following sections will be to determine the conditions on Λ required to achieve maximum power transfer, to derive expressions for the coupling coefficients, and to determine the coupling lengths associated with the power exchange.

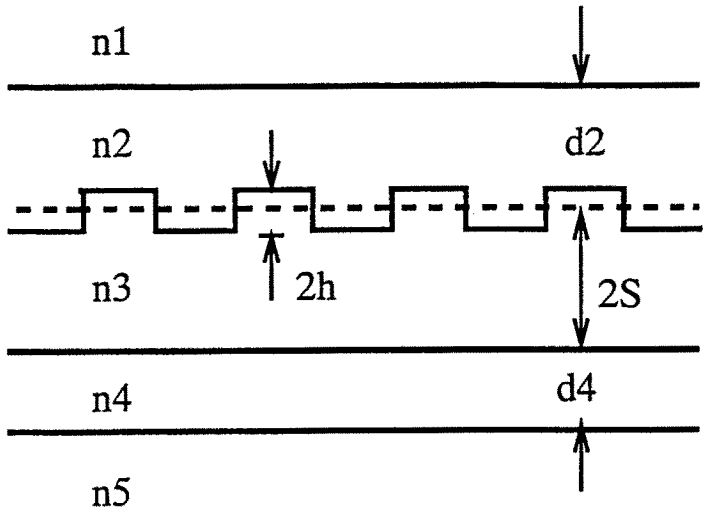

Figure 10. A schematic diagram of a grating-assisted coupler composed of slab waveguides.

A typical two guide slab coupler with a surface corrugation on one of the waveguide boundaries is shown in Fig. 10. In the previous section it was found that for this parallel coupler in the absence of the grating, maximum power transfer occurs when the modes are synchronous, or phase-matched according to

$$(\beta_1 + \kappa_{11}) - (\beta_2 + \kappa_{22}) = 0, \tag{51}$$

where $\beta_{1,2}$ are the propagation constants of the isolated guides, and $\kappa_{11,22}$ are the corrections due to the proximity of the neighboring channel. When the guides are not synchronous, one may expect to intuitively modify (51) by matching the grating frequency, $\Omega = 2\pi/\Lambda$, to the difference in propagation constants

$$(\beta_1 + \kappa_{11}) - (\beta_2 + \kappa_{22}) = \frac{2\pi}{\Lambda}. \tag{52}$$

This phase-matching condition will in general not lead to complete power exchange, since in addition to the grating, the two waveguide modes are also simultaneously coupled through natural or evanescent

coupling. If the waveguides are also closely coupled, then the mode nonorthogonality may additionally modify the phase-matching requirement. For the parallel system, the two modes which are completely decoupled are the even and odd array modes. It is the matching of these, as shown by Marcuse [95], which determine the correct grating period,

$$\beta_s - \beta_a = \frac{2\pi}{\Lambda}. \tag{53}$$

It will be shown that the NCMT yields essentially the same result, in addition to specifying two unique coupling lengths associated with the power transfer.

3.2 Grating Coupling Formulation

For the grating-assisted couplers, the refractive index may be expressed as

$$n^2(x,y,z) = \bar{n}^2(x,y) + \Delta n^2(x,y) f(z), \tag{54}$$

where $\bar{n}$ is the refractive index of the uniform (i.e., z-invariant) reference structure, $\Delta n^2(x,y)$ represents the transverse distribution of the perturbation, and $f(z)$ is the periodic longitudinal distribution. The boundary of the reference structure in the neighborhood of the grating is chosen to lie along the average value of the corrugation, (as seen by the dashed boundary in Fig. 10). This is the optimum choice, since the perturbation will then only generate purely 'AC' varying coupling terms, with no additional uniform or 'DC' coupling component. Because the waveguiding structure is nonuniform, one can not take advantage of the variational expression for the propagation constant, as was done in section 2 for the parallel coupler. Instead, a complex power theorem is employed [59],

$$\frac{d}{dz}\int \{\mathbf{E}_a^* \times \mathbf{H}_b + \mathbf{E}_b \times \mathbf{H}_a^*\} \cdot \hat{z} da = -j\omega \int (\epsilon_a - \epsilon_b)\mathbf{E}_a^* \cdot \mathbf{E}_b da, \tag{55}$$

which relates two lossless index distributions ϵ_a and ϵ_b, and their associated electromagnetic fields.

The total field is assumed to be a superposition of the waveguide modes as in (4). We identify the distribution ϵ_a and electric field $\mathbf{E}_a$ with the dielectric constant and electric field of waveguide i in the absence of both periodic perturbations and other waveguides. $\mathbf{E}_b$ is

chosen as the total field, here as a superposition of waveguide modes, and $\epsilon_b = n^2$ is the actual dielectric constant. Inserting these fields into (55), the following coupled mode equations are established,

$$\mathbf{P}\frac{d}{dz}\mathbf{A} = -j\mathbf{H}\mathbf{A} - j\tilde{\mathbf{K}}\mathbf{A}. \tag{56}$$

The power matrix $\mathbf{P}$, and the uniform coupling matrix $\mathbf{H}$ are identical to those derive in (7) and (8) respectively. The additional coupling terms in $\tilde{\mathbf{K}}$ are due to the periodic modulation, and in component form are

$$\tilde{K}_{ij} = \frac{1}{4}\omega\epsilon_o f(z)\int_{\Delta n}\Delta n^2 \mathbf{e}_i^* \cdot \mathbf{e}_j da, \tag{57}$$

where the integral is evaluated over the perturbed region.

Since $\mathbf{P}$ and $\mathbf{H}$ are independent of z, they may be diagonalized using the procedure outlined in section (3.5). By applying the transformation (34), the equivalent set of coupled equations for the compound modes are obtained

$$\frac{d}{dz}\mathbf{W} = -j[\beta_{s,a}]\mathbf{W} - j\mathbf{L}\mathbf{W}. \tag{58}$$

The vector $\mathbf{W}$ contains the amplitudes of the compound modes. $[\beta_{s,a}]$ is the diagonal matrix containing the propagation constants, which for a two guide coupler, have the analytic forms found in (30). The grating now couples the compound modes through the terms in $\mathbf{L}$, where

$$\mathbf{L} = \mathbf{O}^+\tilde{\mathbf{K}}\mathbf{O}, \tag{59}$$

and $\mathbf{O}$ is the transformation matrix (38). By using (34) and (39), an alternate expression is shown to be

$$L_{ij} = \frac{1}{4}\omega\epsilon_o f(z)\int \Delta n^2 \mathbf{e}_i^* \cdot \mathbf{e}_j da, \tag{60}$$

where $\{i,j\} = \{s,a\}$ are for the even and odd array modes, which may be expressed as summations of the waveguide modes (39). If the exact array modes can be computed, using these in (60) gives a more accurate coupling value [95–102]. If the superposition of waveguide modes are used to express $\mathbf{e}_s$ and $\mathbf{e}_a$, then it is seen that the NCMT gives more accurate values for L_{ij} than the OCMT, for as discussed in section

(3.5), the fields represented by the NCMT correspond more closely to the true fields than those derived from the OCMT, (see Figs. 5 and 6). This distinction can become important in the small region over which the overlap integral is evaluated.

At this point it is instructive to examine the coupling expression L_{sa} when expressed in terms of the waveguide coupling coefficients $\tilde{K}_{ij}$ in (57). Explicitly,

$$L_{sa} = L_{as} = \frac{1}{\cos^2(\alpha)} \left[\frac{\tilde{K}_{22}}{2} \sin(\phi - \alpha) - \frac{\tilde{K}_{11}}{2} \sin(\phi + \alpha) + \tilde{K}_{12} \cos(\phi) \right], \tag{61}$$

where $\tilde{K}_{11}$ and $\tilde{K}_{22}$ are the self-coupling of the waveguide modes, and $\tilde{K}_{12} = \tilde{K}_{21}$ is the cross coupling. The mode detuning is represented in terms of ϕ (from (33)), while α accounts for the nonorthogonality (from (19)). In many solutions of the grating problem, both $\tilde{K}_{11}$ and $\tilde{K}_{22}$ are typically neglected because they apparently seem phase-mismatched when equation (56) for the waveguide mode coupling is examined. However, it is seen from their appearance in (61) that they are indeed phase-matched, (L_{sa} contains the total implicit z-dependence of $f(z)$). This can also be understood in a different perspective by realizing that it is the self-coupling terms which give rise to the so called space harmonics, which phase match the two guides.

If for definitiveness we set $\beta_1 > \beta_2$, then ϕ is positive. It is then apparent in L_{sa} that the self-coupling term $\tilde{K}_{11}$ subtracts from the overall coupling strength of L_{sa}, while $\tilde{K}_{22}$ adds to the strength. Hence for a given grating, the maximum effectiveness is achieved by placing it where $\tilde{K}_{22}$ is large, i.e., on the guide with the smaller propagation constant. This may be explained by noting that for asynchronous guides, the zero crossing of the odd mode field amplitude occurs closer to the guide with the larger propagation constant.

3.3 Solutions to the Grating Coupled Equations

In the foregoing analysis $f(z)$ represented an arbitrary longitudinally periodic profile. This profile may be represented as the Fourier

series

$$f(z) = \sum_{m=-\infty}^{+\infty} F_m e^{-j\frac{2\pi m}{\Lambda}z}. \tag{62}$$

Only one of the m components will cause appreciable (guided mode to guide mode) coupling, and we will assume that this component is the first order, $m = \pm 1$, component. For a sinusoidal perturbation, $F_1 = F_{-1}^* = j1/2$ while for a square profile, $F_1 = F_{-1}^* = j1/\pi$, (the overall amplitude is contained in Δn^2). We derive a transfer matrix that links the amplitudes for the composite modes between two positions along z. From (58)

$$\mathbf{W}(z) = \mathbf{T}_W(z)\mathbf{W}(0), \tag{63}$$

where explicitly

$$t_{11}^W = [\cos(Qz) - j\cos(\eta)\sin(Qz)]e^{-j\frac{\pi}{\Lambda}z}, \tag{64a}$$

$$t_{12}^W = \sin(\eta)\sin(Qz)e^{-j\frac{\pi}{\Lambda}z}, \tag{64b}$$

$$t_{21}^W = -\sin(\eta)\sin(Qz)e^{j\frac{\pi}{\Lambda}z}, \tag{64c}$$

$$t_{22}^W = [\cos(Qz) + j\cos(\eta)\sin(Qz)]e^{j\frac{\pi}{\Lambda}z}. \tag{64d}$$

Q is the coupling strength

$$Q = \sqrt{\delta_W^2 + \kappa_W^2}, \tag{65}$$

and η includes the grating detuning

$$\tan(\eta) = \frac{\kappa_W}{\delta_W}. \tag{66}$$

The detuning factor which measures the degree of asynchronisity between the grating frequency and the difference in propagation constants is

$$\delta_W = \frac{\beta_s - \beta_a}{2} - \frac{\pi}{\Lambda}. \tag{67}$$

The coupling strength for a square grating is found from (60) to be

$$\kappa_W \equiv L_{sa} = \frac{1}{2\pi}\omega\epsilon_o \int \Delta n^2 \mathbf{e}_s^* \cdot \mathbf{e}_a da. \tag{68}$$

The phase-matching condition $\delta_W = 0$ yields the optimum grating period

$$\Lambda_W = \frac{\pi}{\beta_s - \beta_a}. \tag{69}$$

Although Λ_W leads to complete transfer of power for the array modes, it also leads to complete transfer for the waveguide modes. The length over which complete exchange occurs however, may be different between the array and waveguide modes, as will be shown. If the two waveguides are highly dissimilar and also weakly coupled, the natural coupling between the two waveguides may be neglected so that Eq. (69) reduces to

$$\Lambda_A = \frac{\pi}{\beta_1 - \beta_2}. \tag{70}$$

Comparisons between the two phase-matching conditions in (69) and (70) are made for a grating-assisted coupler consisting of slab waveguides. The parameters in Fig. 10 are $n_1 = 1.0$, $n_2 = 3.3$, $n_3 = 3.2$, $n_4 = 3.5$, $n_5 = 3.0$, $d_2 = 1.0\mu m$, $d_4 = 0.3\mu m$. The wavelength is $\lambda = 1.5\mu m$. The grating is placed along the core-cladding interface of the upper slab (Fig. 10). Figure 11 illustrates the grating periods predicted by the two different phase-matching conditions (Λ_W : dash; Λ_A : dash-dot) as functions of the waveguide separation. The phase-matching grating period predicted based on the composite modes in (69) increases as the separation becomes larger, whereas the one based on the waveguide modes in (70) is independent of the separation. These two grating periods are quite different when the two waveguides are close, and (70) is valid only if the separation is very large. For the sake of comparison, we also plotted the grating period calculated based on the exact composite modes (solid). It is seen that the nonorthogonal CMT indeed produces very accurate results for the grating period.

Under the phase-matching condition (69), the transfer matrix becomes

$$\mathbf{T}_W = \begin{pmatrix} \cos(\kappa_W z)e^{-j\frac{\pi}{\Lambda}z} & \sin(\kappa_W z)e^{-j\frac{\pi}{\Lambda}z} \\ -\sin(\kappa_W z)e^{+j\frac{\pi}{\Lambda}z} & \cos(\kappa_W z)e^{+j\frac{\pi}{\Lambda}z} \end{pmatrix}. \tag{71}$$

At the input and output, the amplitudes of the composite modes should be related to those of the waveguide modes so that the power exchange between the waveguides may be examined.

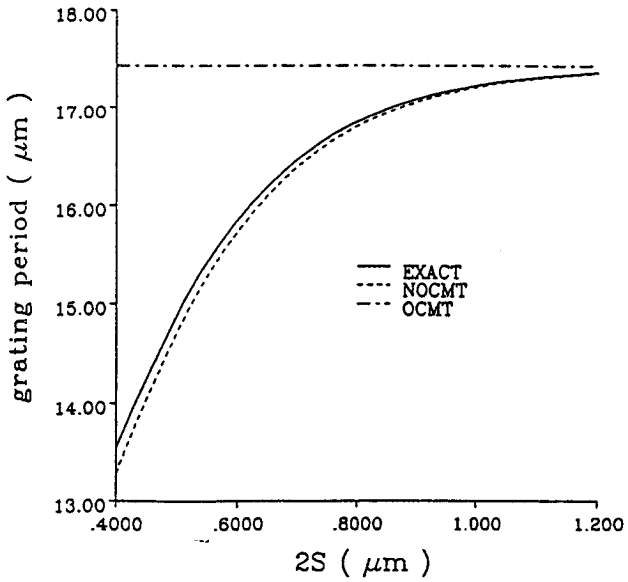

Figure 11. The phase-matching periods as functions of separation for the TE modes of a slab coupler. The parameters are $n_1 = 1.0$, $n_2 = 3.3$, $n_3 = 3.2$, $n_4 = 3.5$, and $n_5 = 3.0$, $d_2 = 1.0\mu m$, $d_4 = 0.3\mu m$, $2S = 0.6\mu m$. $\lambda = 1.5\mu m$. Solid: FD-BPM; dash: NCMT; dash-dot: convention OCMT.

Let the coupling length for complete power exchange of the composite modes be $L_c = N\Lambda$ where L_c is an integer number of grating periods. The transfer matrix for the amplitudes of the waveguide modes is

$$\mathbf{T}_A = \mathbf{O}\mathbf{T}_W\mathbf{O}^{-1} = \frac{1}{\cos(\alpha)} \begin{pmatrix} \cos(\kappa_W L_c - \alpha) & \sin(\kappa_W L_c) \\ -\sin(\kappa_W L_c) & \cos(\kappa_W L_c + \alpha) \end{pmatrix}. \tag{72}$$

Suppose that at the input only guide 1 is excited. The guided powers in guide 1 and 2 are given by

$$P_1(L_c) = \cos^2(\kappa_W L_c), \tag{73a}$$

$$P_2(L_c) = \sin^2(\kappa_W L_c - \alpha). \tag{73b}$$

Complete power transfer occurs at

$$L_{max} = \frac{\pi/2 + \alpha}{\kappa_W}, \tag{74}$$

which differs from that predicted by the conventional OCMT by the presence of α. According to the NCMT, the maximum power transfer length is related to the coupling between the composite modes as well as to the cross-power between the two guides. Zero cross-talk in guide 1 may also be achieved at a different coupling length

$$L_{min} = \frac{\pi}{2\kappa_W}. \tag{75}$$

The power coupling in the grating-assisted coupler is calculated by using the nonorthogonal coupled-mode formulations developed above and the results are shown in Figs. 12a and 12b by dashed curves. The same structure as used in Fig. 11 is assumed. The separation between the two slabs is $2s = 0.6\mu m$ and represents a closely coupled situation. The height of the grating is $2h = 0.1$ and $0.2\mu m$ in Figs. 12a and 12b, respectively. The two distinct coupling scales are clearly illustrated in both cases. The slow scale, which dictates the overall power coupling, is determined by the coupling of the grating. The fast scale is due to the natural coupling between the two parallel uniform waveguides. The period of the fast oscillation is equal to Λ and its magnitude is related to the strength of the natural coupling between the two waveguides. If the two waveguides are far from synchronism and far apart, then the natural coupling may be ignored.

To assess the accuracy of the coupled-mode theory, we have also simulated the same structure by using a beam propagation method [65] (solid curves). Better agreement between the two methods is observed for the case in Fig. 12a than for Fig. 12b. When the grating perturbation is strong, the trial solutions in the CMT are no longer accurate, resulting in larger errors. In addition, the radiation loss becomes more pronounced as the grating height increases. This is illustrated in the BPM simulations, but is absent in the coupled-mode analysis derived here. Radiation can be incorporated into the coupled-mode framework by considering guide mode to radiation mode coupling [16,104,105].

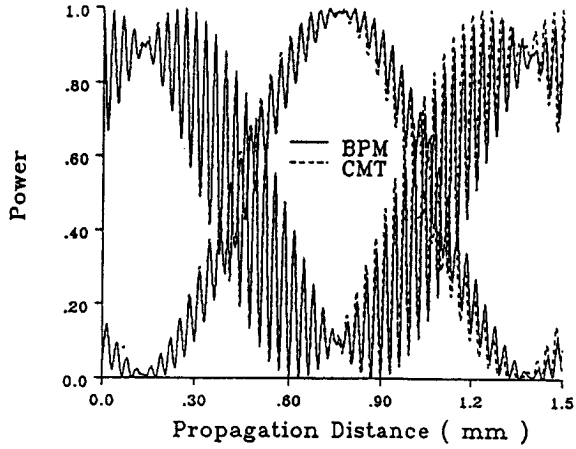

(a)

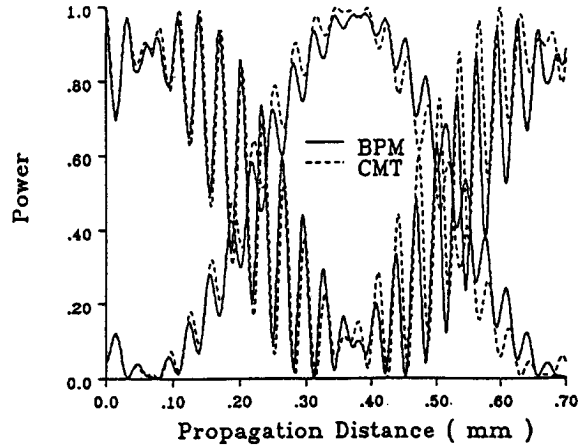

(b)

Figure 12. Power exchange as a function of z. Solid: FD-BPM; dash: NCMT. (a) $2h = 0.1\mu m$; (b) $2h = 0.2\mu m$. The parameters are the same as in Figure 11.

4. Tapered Directional Couplers

In this section a taper is defined as a coupled section of waveguide where the separation between two waveguides varies with the propagation distance z. In this situation the uniform evanescent coupling will vary with propagation distance. Further, this nonuniformity will give rise to an additional coupling component due purely to the nature of the z-variation. A typical tapered section which may be found at the output of a parallel coupler is depicted in Fig. 13.

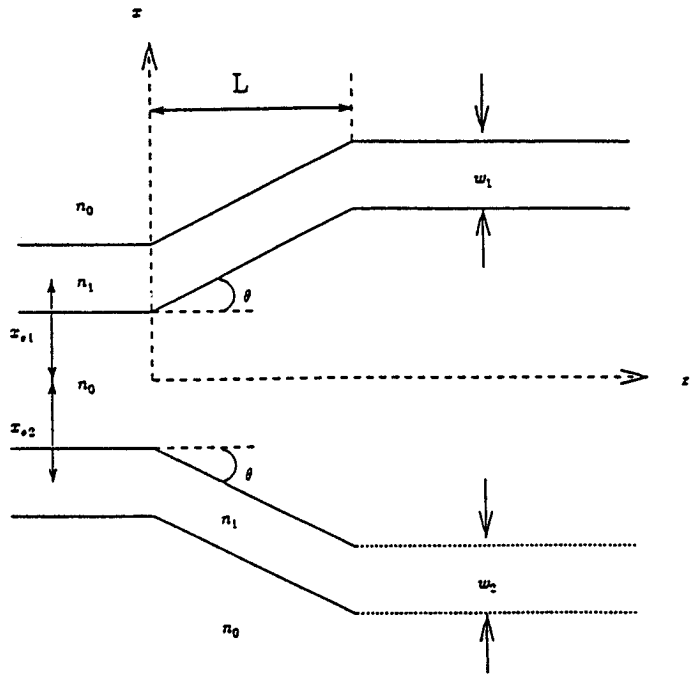

Figure 13. A nonparallel or tapered section of waveguide at the output of a directional coupler.

The coupling characteristics of the taper are of fundamental importance, since tapers often serve as input and output sections, bringing two isolated waveguides into close proximity or carrying power

away from a coupled region. A taper also serves as a signal processing element for applications such as: spectral bandpass shaping, spectral sidelobe suppressing, for reducing fabrication tolerances, and to eliminate channel cross talk. Since the overall performance of a coupled device can often be critically affected by the characteristics of the nonparallel sections, it is important to undertake a rigorous analysis of the power exchange in tapered waveguide structures using the most recent coupled-mode formulations.

The early work of coupled-mode theory for tapered structures was pioneered by Cook, Fox, and Louisell [10108] in a series of papers dated in 1955, for the topic of transmission lines, and later by Matsuhara [109] *et. al.*, with extension to optical waveguides. The value of side lobe suppression in the frequency domain, and cross-talk reduction in neighboring channels, were expressed first by Alferness [17,110], and then by others [111,112], both theoretically and with experimental confirmation.

In the earlier formulations, the simple theory of coupling of power-orthogonal waveguide modes had been used, with coupling due to the taper taken into account by simply making the uniform coupling coefficients functions of z. There has been an effort to extend the nonorthogonal coupled-mode formulations for the parallel waveguides to the nonparallel cases [68–70,72,113,114]. Inconsistencies arise, however, if one simply attempts to add a z-varying nonorthogonality without considering the additional coupling component arising independently from the varying nature of the coupling. In many reformulations, power conservation had been violated [68,113,114]. A scalar nonorthogonal coupled-mode theory that conserves power to within its level of approximation was proposed by Peall and Syms [69], and most recently a self-consistent vector theory by Huang and Haus [70,72]. The additional effect of wavefront tilt and the taper-to-uniform coupler junction discontinuity, has also recently been addressed [74].

4.1 Nonorthogonal Coupled-Mode Formulations

The total electromagnetic fields in the structure obey Maxwell's equations, which we write as

$$\hat{\mathbf{z}} \times \frac{\partial \mathbf{E}}{\partial z} + \nabla_t \times \mathbf{E} = -j\omega\mu_o \mathbf{H}, \tag{76a}$$

$$\hat{\mathbf{z}} \times \frac{\partial \mathbf{H}}{\partial z} + \nabla_t \times \mathbf{H} = j\omega\epsilon \mathbf{E}. \tag{76b}$$

As usual, the total fields are expressed as summations of the waveguide modes

$$\mathbf{E} = \sum a_i(z)\mathbf{e}_i(x, y; z), \tag{77a}$$

$$\mathbf{H} = \sum a_i(z)\mathbf{h}_i(x, y; z). \tag{77a}$$

The fields $\mathbf{e}_i$ and $\mathbf{h}_i$ are local modes which are defined at some cross section z. They obey (5) locally (i.e., they behave as z-invariant modes).

The expansion (77) is a good approximation if local guided modes exist in the entire coupling region and the two waveguides are not very closely coupled and/or strongly guided. We also assume that the taper varies slowly so that the coupling to the radiation modes and/or the effect of wavefront tilt may be neglected.

The coupled-mode equations governing the evolution of the expansion coefficients $a_1(z)$ and $a_2(z)$ can be derived by substituting (77) into Maxwell's equations [72]. In matrix form, the equations are written as

$$\mathbf{P}\frac{d}{dz}\mathbf{A} = -j\mathbf{H}\mathbf{A} - \mathbf{F}\mathbf{A}, \tag{78}$$

where H_{ij} and P_{ij} are the same as those defined in (7) and (8). Note that for tapered couplers they become z-dependent. In addition, a new coupling term appears in the coupled-mode equations

$$F_{ij} = \frac{1}{4}\int (\mathbf{e}_i^* \times \frac{\partial \mathbf{h}_j}{\partial z} + \frac{\partial \mathbf{e}_j}{\partial z} \times \mathbf{h}_i^*) \cdot \hat{z}\, da, \tag{79}$$

representing the additional coupling caused by the taper. An alternate expression may be derived in terms of the cross power, as is readily verified

$$F_{ij} = \frac{1}{2}\frac{dP_{ij}}{dz} = \frac{1}{2}\frac{d\alpha}{dz}\cos(\alpha). \tag{80}$$

Since $P_{11,22}$ are normalized to unity this implies that $F_{11,22} = 0$. This may also be verified by applying power conservation, since the F_{ij} are real valued. It has been shown that F_{ij} are essential for self-consistency of nonorthogonal coupled-mode equations [72,73]. Even for a very slow taper, F_{ij} should not be adiabatically neglected, otherwise power conservation will be violated. It will be shown later that a self-consistent adiabatic approximation for slowly tapered couplers may be introduced in conjunction with the orthogonal coupled-mode formulation based on the local composite modes.

4.2 Power-Orthogonal Mode Formulations

The power-orthogonalized coupled-mode formulation carried out in section (3.4) has a useful role when treating z-varying structures. In that section the waveguide modes are orthogonalized by the transformation $\mathbf{B} = \mathbf{QA}$, with the transformation matrix $\mathbf{Q}$ defined in (19). By applying the transformation on (78), the evolution of the power-orthogonal modes follow

$$\frac{d}{dz}\mathbf{B} = -j\mathbf{H}'\mathbf{B} - \mathbf{F}'\mathbf{B}, \tag{81}$$

where $\mathbf{H}'$ is identical with (22) except now the elements vary with z. The coupling due to the taper is

$$\mathbf{F}' = (\mathbf{Q}^+)\mathbf{F}\mathbf{Q} - (\frac{d}{dz}\mathbf{Q})\mathbf{Q}^{-1} \tag{82}$$

By carrying out the algebraic manipulations in (82), and using the expression for $\mathbf{F}$ in (80), it is found that $\mathbf{F}'$ is identically zero. Hence

$$\frac{d}{dz}\mathbf{B} = -j\mathbf{H}'\mathbf{B}, \tag{83}$$

and the power-orthogonal modes are found to be in adiabatic form.

4.3 Normal Mode Formulation

The coupled-mode equations for the local normal modes can be derived from (78) by the linear transformations in (34)–(38). In matrix form, these are reduced to

$$\frac{d}{dz}\mathbf{W} = -j\mathbf{B}\mathbf{W} - \mathbf{N}\mathbf{W}, \tag{84}$$

where the local composite modes are given in terms of the linear superposition of the local waveguide modes determined by (39). The coupling coefficients are obtained as

$$\mathbf{N} = \mathbf{O}^+\mathbf{P}\frac{d}{dz}\mathbf{O} + \mathbf{O}^+\mathbf{F}\mathbf{O}. \tag{85}$$

By imposing the condition for power conservation, one can easily prove that the coupling coefficients are antisymmetric, i.e,

$$N_{sa} = -N_{as}^*, \tag{86}$$

and the diagonal elements $N_{ss} = N_{aa} = 0$. This result is to be expected : since the coupling matrix in (85) is real, its diagonal elements must be zero; otherwise power would be lost or generated and thus power conservation would be violated. It is also evident that the additional coupling terms F_{ij} are essential to ensure the self-consistency of the coupled-mode formulation.

The orthogonal coupled-mode equations (84) can also be derived from Maxwell's equations when the fields in the tapered coupler are represented by the linear superposition of the exact local normal modes [72,115,116]. The coupling coefficients result solely from the tapering effect and are given by

$$N_{sa} = \frac{1}{4}\int (\mathbf{e}_s^* \times \frac{\partial \mathbf{h}_a}{\partial z} + \frac{\partial \mathbf{e}_a}{\partial z} \times \mathbf{h}_s^*) \cdot \hat{z} da, \tag{87}$$

where $\mathbf{e}_{s,a}$ and $\mathbf{h}_{s,a}$ are the fields of the local composite modes. By using the linear transformation (34) and (39), one may readily derive (87) from (85). The evaluation of the coupling coefficients between the local composite modes using (85) or (87) is cumbersome. An alternative expression for the coupling coefficient may be derived [24]

$$N_{sa} = \frac{1}{4}\frac{\omega\epsilon_o}{\beta_s - \beta_a}\int \frac{\partial n^2}{\partial z}\mathbf{e}_s^* \cdot \mathbf{e}_a da, \tag{88}$$

Note that the coupling between the local composite modes is proportional to the rate of change in the refractive index along z. If the taper is very slow, then the coupling between the local composite modes may be neglected and a self-consistent coupled-mode formulation under the adiabatic approximation is obtained. In general, however, the coupling due to taper should be considered and its effect on the power exchange between the guides should be carefully examined.

4.4 Power Exchange in the Tapered Couplers

For synchronous couplers in which the local modes of the waveguides have the same propagation constant, there is no coupling between the local composite modes, i.e., $N_{sa} = 0$. Thus, (84) can be integrated to yield exact solutions [69]. By assuming $a_1(0) = 1$ and $a_2(0) = 0$, the mode amplitudes at z may be expressed as

$$a_1(z) = \frac{1}{2}\left[\sqrt{\frac{1-X(0)}{1-X(z)}} + \sqrt{\frac{1+X(0)}{1+X(z)}}\right]\cos\left(\frac{1}{2}\phi\right) + j\frac{1}{2}\left[\sqrt{\frac{1-X(0)}{1-X(z)}} - \sqrt{\frac{1+X(0)}{1+X(z)}}\right]\sin\left(\frac{1}{2}\phi\right), \tag{89a}$$

$$a_2(z) = \frac{1}{2}\left[\sqrt{\frac{1-X(0)}{1-X(z)}} + \sqrt{\frac{1+X(0)}{1+X(z)}}\right]\cos\left(\frac{1}{2}\phi\right) - j\frac{1}{2}\left[\sqrt{\frac{1-X(0)}{1-X(z)}} - \sqrt{\frac{1+X(0)}{1+X(z)}}\right]\sin\left(\frac{1}{2}\phi\right), \tag{89b}$$

where

$$\phi = \int_0^z \left(\frac{\beta_s - \beta_a}{2}\right)dz', \tag{90}$$

$X(z)$ is the cross power at some position z, and $\beta_{s,a}$ are the propagation constants of the symmetric and the antisymmetric local composite modes given by (30).

When the waveguides are not synchronous, exact analytical solutions are known only for certain cases where some special relations among β_s, β_a and N_{sa} hold [27]. In general, the coupled-mode equations may be solved by using a numerical technique. If the two guides are very far apart at $z = L$, the cross-power $X(L)$ may be neglected so that

$$P_1(L) \approx |a_1(L)|^2, \tag{91a}$$

$$P_2(L) \approx |a_2(L)|^2. \tag{91b}$$

Therefore the cross-talk between the two guides may be greatly reduced by introducing a tapered section in the output port of the directional couplers [86].

To examine the power coupling in a tapered coupler, we studied a coupler made of two straight step-index slab waveguides separating at an angle 2θ (as in Fig. 13). The input conditions are assumed to be $a_1(0) = 1$ and $a_2(0) = 0$. The parameters of the waveguides are $n_1 = n_2 = 3.1$, $n_0 = 3.0$, $w_1 = 0.8\mu m$ and $w_2 = 0.6\mu m$. The initial separation between the slab centers is $x_{o1} = 0.55\mu m$ and

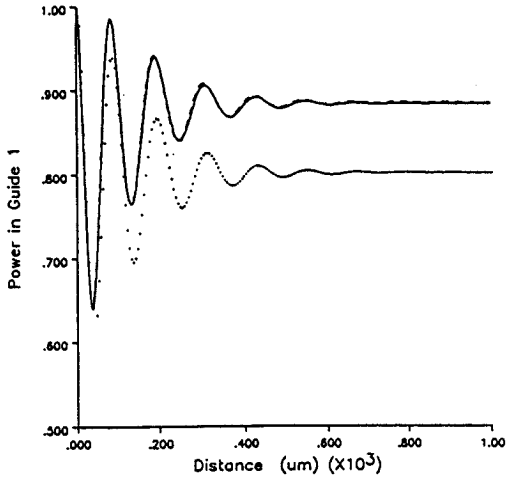

(a)

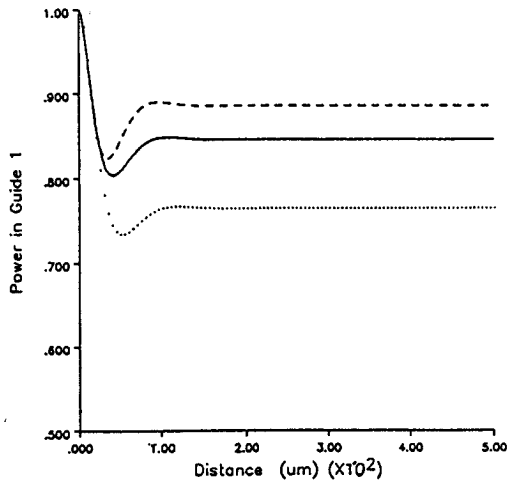

(b)

Figure 14. The guided power in guide 1 as a function of the taper length L in Figure 13. The parameters are $n_1 = n_2 = 3.1$, $n_0 = 3.0$, $w_1 = 0.8\mu$ and $w_2 = 0.6\mu m$. $x_{o1} = 0.55\mu m$ and $x_{o2} = 0.45\mu m$. The wavelength is $\lambda = 1.5\mu m$. (a)$\theta = 0.1°$; (b)$\theta = 0.5°$. Solid: Nonorthogonal CMT with tapering effect; dash: Nonorthogonal CMT that neglects N_{sa}; dot: Nonorthogonal CMT that neglects F_{12}.

$x_{o2} = -0.45\mu m$, and the wavelength is $\lambda = 1.5\mu m$. Figures 14a and 14b show the guided power in guide 1 as a function of the taper length L for two tilt-angles $\theta = 0.1°$ and $0.5°$, respectively. The solid curves represent the solutions including the tapering effect, the dash curves are for the solutions under adiabatic approximation (neglecting N_{sa}), and the dotted curves are for the solutions that simply neglect F_{ij}. When the tilt-angle is small, the adiabatic solutions appear to be accurate. As the angle increases (as in Fig. 14b), the tapering effect becomes important and the adiabatic solutions are no longer adequate. The solutions that ignore F_{ij} are not correct even when the tilt angle is small. A closer examination reveals that the solutions in fact do not obey the power conservation and thereby are not self-consistent.

5. Vector Properties of Couplers

The coupled-mode formulations developed in the previous sections used the vector modes of the individual waveguides as the trial solutions for the complete field. If the index discontinuities are large however, this trial solution may become inaccurate in describing the vector property of the entire coupler. This issue was first raised by Snyder and coworkers [35,36,43], where they showed that erroneous results are obtained for the TM coupling length of couplers with large discontinuities. It is clear in this case that the error arises because the proper field discontinuity across the index boundaries will not be preserved.

Consider for instance, TM mode coupling in the parallel arrangement. If the total electric field is described as a superposition of waveguide modes as in (4), then the evanescent tail of mode 1 is continuous across the boundaries of guide 2. Hence the proper discontinuity of the total field across the boundary is in error. This will cause errors in the evaluation of the overlap integrals. If the index discontinuities are large, then one should use a new set of modified trial solutions [44]

$$\mathbf{e}_1' = \mathbf{e}_1 + \delta\mathbf{e}_1, \tag{92a}$$

$$\mathbf{e}_2' = \mathbf{e}_2 + \delta\mathbf{e}_2, \tag{92b}$$

where $\mathbf{e}_{1,2}$ are the individual modal fields satisfying Maxwell's equations for their respective waveguides, and the corrections $\delta\mathbf{e}_1$ and $\delta\mathbf{e}_2$ are nonzero only inside the cores of guides 2 and 1 respectively. To

find their magnitudes, we will attempt to force the correct discontinuity across the core boundaries. Consider TM modes in the symmetric directional coupler of Fig. 1, where we set $n_1 = n_3 = n_5 = n_{cl}$ for the claddings, and $n_2 = n_4 = n_{co}$ for the cores. At the inner boundary of guide 2, the total field on either side of $x = S$ satisfies

$$\mathbf{E}(S^-) = \frac{n_{co}^2}{n_{cl}^2}\mathbf{E}(S^+). \tag{93}$$

Substituting for the component modes

$$a_1\mathbf{e}_1(S^-) + a_2\mathbf{e}_2(S^-) = \frac{n_{co}^2}{n_{cl}^2}\left[a_1\mathbf{e}_1(S^+) + \delta a_1\mathbf{e}_1 + a_2\mathbf{e}_2(S^+)\right]. \tag{94}$$

Since $\mathbf{e}_2(S^-) = n_{co}^2/n_{cl}^2\mathbf{e}_2(S^+)$ is already satisfied, then

$$\delta\mathbf{e}_1 = \left(\frac{n_{cl}^2}{n_{co}^2} - 1\right)\mathbf{e}_1(S). \tag{95a}$$

The correction $\delta\mathbf{e}_2$ is likewise found to be

$$\delta\mathbf{e}_2 = \left(\frac{n_{cl}^2}{n_{co}^2} - 1\right)\mathbf{e}_2(-S). \tag{95b}$$

By substituting the corrected fields into the variational expression for the propagation constant (3), the following modified coupling coefficients result

$$H'_{ij} = P'_{ij}\beta_j + \kappa'_{ij} + (\beta_i - \beta_j)\delta P_{ij}, \tag{96a}$$

$$\kappa'_{ij} = \kappa_{ij} + \frac{1}{4}\omega\int[\bar{n}^2 - n_i^2]\{\delta\mathbf{e}_i^* \cdot \mathbf{e}_j + \mathbf{e}_i^* \cdot \mathbf{e}_j\}da$$

$$- j\frac{1}{4}\omega\int\bar{n}^2\delta\mathbf{e}_i^*\delta\mathbf{e}_j da, \tag{96b}$$

$$P'_{ij} = P_{ij} + \frac{1}{4}\int[\delta\mathbf{e}_i^* \times \mathbf{h}_j + \delta\mathbf{e}_j \times \mathbf{h}_i^*] \cdot \hat{\mathbf{z}}da \tag{96c}$$

$$\delta P_{ij} + \frac{1}{4}\int\delta\mathbf{e}_j \times \mathbf{h}_i^* \cdot \hat{\mathbf{z}}da \tag{96d}$$

Note that in the derivation of these expressions $\mathbf{e}_i$, and not $\mathbf{e}_i'$, satisfy Maxwell's equations for the waveguide modes (5), and hence the results are not obtained simply from substituting $\mathbf{e}_i'$ into the original coefficients (7)–(9).

The foregoing method of improving the trial solutions was straight forward and simple. This will not be the case in general for more complicated structures. To date there have been two avenues of approach to deal systematically with the polarization issue. One possibility is to use the scalar formulation and apply a vector correction [25,50]. Alternatively, Yasumoto [117] has shown the possibility of setting up a perturbation approach to the solution which satisfies the boundary conditions at each perturbation order.

In Figures 15a and 15b, we examine the dispersion characteristics of a weakly coupled TM mode slab coupler, taken from [44]. The waveguide parameter V is chosen as $V = 1$, while the distance between the core centers is $4d$, with d being the guide thickness. The physics of power transfer is related to the beat length, the difference between the even and odd propagation constants $(\beta_s - \beta_a)$ as in (43). In Fig. 15a we plot the percentage of error between $(\beta_s - \beta_a)$ as calculated by the NCMT compared to that calculated from the exact compound modes. The three curves plotted represent the NCMT based on the TM slab modes (dash), the NCMT with field corrections (dash-dot), and the conventional CMT neglecting both cross-power and self coupling. The uncorrected NCMT departs significantly from the exact values for index steps larger than 1.5, while the corrected NCMT is valid up to a index steps of 2.5. What is surprising is that the conventional CMT is superior to the NCMT at larger step discontinuities. On the other hand, we examine the individual propagation constants β_s and β_a in Fig. 15b as a function of index difference. There it is seen that the corrected NCMT does in fact reproduce the individual dispersion curves quite accurately, and more accurately than the conventional CMT. It should be noted that in this extreme example, the beat length is less than $10\mu m$, and hence the validity of slowly varying amplitudes inherent in the coupled mode theories must be examined more closely.

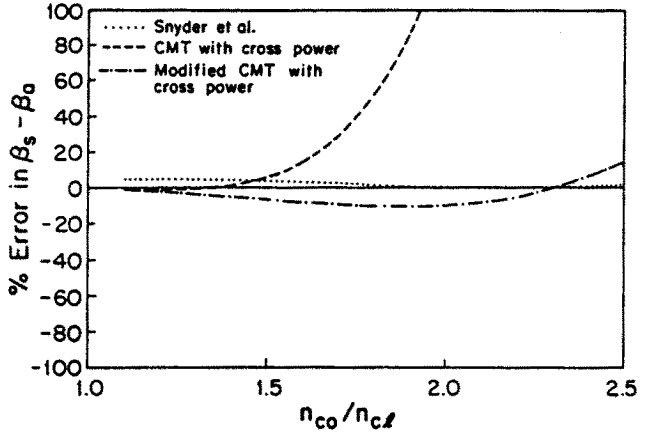

(a)

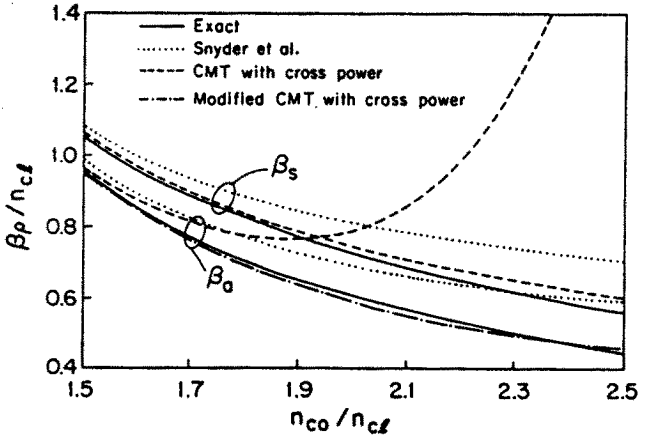

(b)

Figure 15. (a) The percentage error in the coupling lengths predicted by various formulations for the TM modes of a parallel slab coupler. (b) The effective indices of the TM modes of parallel slabs. Taken from Ref. [44].

References

1. Pierce, J. R., "Coupling of modes of propagation," *J. Appl. Phys.*, Vol. 25, 179–183, 1954.
2. Miller, S. E., "Coupled wave theory and waveguide applications," *Bell Syst. Tech. J.*, Vol. 33, 661–719, 1954.
3. Louisell, W. H., "Analysis of the single tapered mode coupler," *Bell Syst. Tech. J.*, Vol. 33, 853-871, 1954.
4. S. A. Schelkunoff, "Conversion of Maxwell's equations into generalized telegraphist's equations," *Bell Syst. Tech. J.*, Vol. 34, 995–1043, 1955.
5. Haus, H. A., "Electron beam waves in microwave tubes," in *Proc. Symp. Electronic Waveguides,* Polytechnic Institute of Brooklyn, 1958..
6. Snyder, A. W., "Coupled mode theory for optical fibers," *J. Opt. Soc. Am.*, Vol. 62, 1267–1277, 1972.
7. Marcuse, D., "Coupled mode theory of round optical fibers," *Bell Sys. Tech. J.*, Vol. 52, 817–842, 1973.
8. Yariv, A., "Coupled-mode theory for guided-wave optics," *IEEE J. Quantum Electron.*, Vol. 9, 919–933, 1973.
9. Kogelnik, H., "Theory of dielectric waveguides," in *Integrated Optics,* T. Tamir, ed., Springer-Verlag, New York, 1975, Chap. 2.
10. Taylor, H. F., "Optical switching and modulation in parallel dielectric waveguides," *J. Appl. Phys.*, Vol. 44, 3257–3262, 1973.
11. Kogelnik, H., "Switched directional couplers with alternating $\Delta\beta$," *IEEE J. Quantum Electron.*, Vol. 12, 39401, 1976.
12. Noda, J., M. Fukuma, and O. Mihami, "Design calculations for directional couplers fabricated by Ti-diffused $LiNbO_3$ waveguides," *Appl. Opt.*, Vol. 20, 2284–2298, 1981.
13. McIntyre, P., and A. W. Snyder, "Power transfer between optical fibers," *J. Opt. Soc. Amer.*, Vol. 63, 1518–1527, 1983.
14. Kogelnik, H., and C. V. Shank, "Coupled-wave theory of distributed feedback lasers," *J. Appl. Phys.*, Vol. 43, 2327–2335, 197).
15. Cremer, C., G. Heise, R. Marz, M. Schienle, G. Shulte-Roth, and H. Unzeitig, "Bragg gratings on InGaAsP/InP waveguides as polarization independent optical filters," *IEEE J. Lightwave Tech.*, Vol. 7, 1641–1645, 1989.
16. Syms, R. R. A., "Optical directional coupler with grating overlay," *Appl. Opt.*, Vol. 24, 717–726, 1985.

17. Alferness, R. C., and P. S. Cross, "Filter characteristics of codirectionally coupled waveguides with weighted coupling," *IEEE J. Quantum Electron.,* Vol. 14, 843–847, 1978.
18. Sakai, J., and T. Kimura, "Birefringence and polarization characteristics of single-mode optical fibers under elastic deformation," *IEEE J. Quantum Electron.,* Vol. QE-17, 1041–1051, 1981.
19. Marcuse, D., "Radiation loss of grating-assisted directional coupler," *IEEE J. Lightwave Technol.,* Vol. 8, 675–684, 1990.
20. Stegeman, G. I., and C. T. Seaton, "Nonlinear integrated optics," *J. Appl. Phys.,* Vol. 58, R57–R78, 1985.
21. Anderson, D. R., S. Datta, and R. L. Gunshor, "A coupled-mode approach to modulation instability and envelope solitons," *J. Appl. Phys.,* Vol. 54, 5608–5612, 1983.
22. Jensen, S. M., "The nonlinear coherent coupler," *IEEE J. Quantum Electron.,* Vol. QE-18, 1580–1583, 1982.
23. Lee, D. L., *Electromagnetic Principle of Integrated Optics,* John Wiley, New York, 1986.
24. Marcuse, D., *Theory of Dielectric Optical Waveguides,* 2nd ed., Academic Press, New York, 1991.
25. Snyder, A. W., and J. D. Love, *Optical waveguide theory,* Chapman and Hall, London and New York, 1983.
26. Haus, H. A., *Waves and Fields in Optoelectronics,* ,Prentice-Hall, Englewood Cliffs, New Jersey, 1984.
27. Tamir, T., Ed., *Guided-Wave Optoelectronics,* Springer-Verlag, New York, 1988.
28. Shen, Y. R., *Principles of Nonlinear Optics,* John Wiley, New York, 1984.
29. Agrawal, G. P., *Nonlinear fiber optics,* Academic Press, Boston, 1989.
30. Hardy, A., and W. Streifer, "Coupled-mode theory of parallel waveguides," *IEEE J. Lightwave Technol.* Vol. LT-3, 1135–1146, 1985.
31. Haus, H. A., W. P. Huang, S. Kawakami, and N. A. Whitaker, "Coupled mode theory of optical waveguides," *IEEE J. Lightwave Technol.,* Vol. LT-5, 123, 1987.
32. Chuang, S. L., "A coupled mode formulation by reciprocity and a variational principle," *IEEE J. Lightwave Technol.,* Vol. 5, 5–15, 1987.

33. Streifer, W., M. Osinski, and A. Hardy, "Reformulation of coupled-mode theory of multiwaveguide systems," *IEEE J. Lightwave Technol.*, Vol. 5, 1–4, 1987.
34. Vassello, C., "About coupled-mode theories for dielectric waveguides," *IEEE J. Lightwave Technol.*, Vol. 6, 294–303, 1988.
35. Snyder, A. W., A. Ankiewicz, and A. Altintas, "Fundamental error of recent coupled mode formulations," *Electron. Lett.*, Vol. 23, 1097–1098, 1987.
36. Snyder, A. W., A. Ankiewicz, and A. Altintas, "Coupled mode theory neglects polarization phenomena," *Electron. Lett.*, Vol. 22, 720–721, 1988.
37. Streifer, W., "Coupled mode theory," *Electron. Lett.*, Vol. 23, 21217, 1987.
38. Streifer, W., "Comment on 'Fundamental error of recent coupled mode formulations'," *Electron. Lett.*, Vol. 22, 718–719, 1988.
39. Snyder, A. W., A. Ankiewicz, "Fibre Couplers composed of unequal cores," *Electon. Lett.*, Vol. 22, 1237–1238, 1988.
40. Streifer, W., M. Osinski, and A. Hardy, "A critical review of coupled mode theory," in *Proc. SPIE*, Integrated Optical Circuit Engineering, Boston, p. 178, 1987.
41. Hardy, A., W. Streifer, and M. Osinski, "Weak coupling of parallel waveguides," *Opt. Lett.*, Vol. 13, 162–163, 1988, Erratum: *Opt. Lett.*, Vol. 13, p. 428, 1988.
42. Wang, Z. H., and S. R. Seshadri, "Asymptotic theory of guided modes in two parallel, identical dielectric waveguides," *J. Opt. Soc. Am.*, Vol. A5, 782–792, 1988.
43. Ankiewicz, A., A. Altintas, and A. W. Snyder, "Polarization properties of evanescent couplers," *Opt. Lett.*, Vol. 13, 524–525, 1988.
44. Haus, H. A., W. P. Huang, and A. W. Snyder, "Coupled-mode formulations," *Opt. Lett.*, Vol. 14, 1222–1224, 1989.
45. Vassallo, C., "Condensed formula for coupling coefficients between parallel dielectric waveguides," *Electron. Lett.*, Vol. 23, 304–306, 1986.
46. Marcatili, E., "Improved coupled-mode equations for dielectric guides," *IEEE J. Quantum Electron.*, Vol. 22, 988–993, 1986.
47. Snyder, A. W., "Optical fiber couplers-optimum solution for unequal cores," *IEEE J. Lightwave Technol.*, Vol. 6, 463–474, 1988.

48. Syms, R. R. A., and R. G. Peall, "Explanation of asymmetric switch response of three-arm directional couplers in Ti:$LiNbO_3$ using strong coupling theory," *Opt. Comm.*, Vol. 66, 260–264, 1988.
49. Huang, W. P., and S. K. Chaudhuri, "Variational coupled-mode theory of optical couplers," *IEEE J. Lightwave Technol.*, Vol. 8, 1565–1570, 1990.
50. Huang, W. P., S. T. Chu, and S. K. Chaudhuri, "A scalar coupled-mode theory with vector correction," *IEEE J. Quantum Electron.*, Vol. 28, 184–193, 1992.
51. Hardy, A., and W. Streifer, "Coupled modes of multiwaveguide systems and phased arrays," *IEEE J. Lightwave Technol.*, Vol. 4, 90–99, 1986.
52. Chuang, S. L., "A coupled-mode theory for multiwaveguide systems satisfying the reciprocity theorem and power conservation," *IEEE J. Lightwave Technol.*, Vol. 5, 174–183, 1987.
53. Hardy, A., and W. Streifer, "Analysis of phased-array diode lasers," *Opt. Lett.*, Vol. 10, 335–337, 1985.
54. Hardy, A., and W. Streifer, "Coupled-mode solutions of multiwaveguide systems," *IEEE J. Quantum Electron.*, Vol. 22, 528–534, 1986.
55. Shama, Y., A. Hardy, E. Marom, "Multimode coupling of unidentical waveguides," *IEEE J. Lightwave Technol.*, Vol. 7, 420–425, 1989.
56. Hardy, A., W. Streifer, and M. Osinski, "Coupled-mode equations for multimode waveguide systems in isotropic or anisotropic media," *Opt. Lett.*, Vol. 11, 742–744, 1986.
57. Tian, F., Y. Z. Wu, and P. A. Ye, "Improved coupled-mode theory for anisotropic waveguide modulators," *IEEE J. Quantum Electron.*, Vol. 24, 531–536, 1988.
58. Tsang, L., and S. L. Chuang, "Improved coupled-mode theory for reciprocal anisotropic waveguides," *IEEE J. Lightwave Technol.*, Vol. 6, 304–311, 1988.
59. Huang, W. P., and H. A. Haus, "Power exchange in grating-assisted couplers," *IEEE J. Lightwave Technol.*, Vol. 7, 920–924, 1989.
60. Huang, W. P., B. E. Little, and S. K. Chaudhuri, "A new approach to grating-assisted couplers," *IEEE J. Lightwave Technol.*, Vol. 9, 721–727, 1991.

61. Huang, W. P., and W. Y. Lit, "Nonorthogonal coupled-mode theory of grating-assisted codirectional couplers," *IEEE J. Lightwave Technol.*, Vol. 9, 845–852, 1991.
62. Little, B. E., W. P. Huang, and S. K. Chaudhuri, "A multiple-scale analysis of grating-assisted couplers," *IEEE J. Lightwave Technol.*, Vol. 10, 1254–1263, 1992.
63. Griffle, G., M. Itzkovich, and A. A. Hardy, "Coupled-mode formulations for directional couplers with longitudinal perturbation," *IEEE J. Quantum Electron.*, Vol. 28, 985–994, 1992.
64. Griffle, G., and A. Yariv, "Frequency response and tunability of grating-assisted directional couplers," *IEEE J. Quantum Electron.*, Vol. 27, 1115–1118, 1991.
65. Huang, W. P., B. E. Little, and C. L. Xu, "On phase-matching and power coupling in grating-assisted couplers," *IEEE Photon. Technol. Lett.*, Vol. 4, 151–153, 1992.
66. Syms, R. R. A., "Improved coupled-mode theory for codirectionally and contradirectionally coupled waveguide arrays," *J. Opt. Soc. Am.*, Vol. A8, 1062–1069, 1991.
67. Hong, J., and W. P. Huang, "Contra-directional coupling in grating-assisted guided-wave devices," *IEEE J. Lightwave Technol.*, Vol. 10, 873–881, 1992.
68. Hardy, A., M. Osiński, and W. Streifer, "Application of coupled-mode theory to nearly parallel waveguide systems," *Electron. Lett.*, Vol. 22, 1249–1250, 1986.
69. Peall, R. G., and R. R. A. Syms, "Scalar strong coupled mode theory for slowly-varying waveguide arrays," *Opt. Comm.*, Vol. 67, 421–424, 1988.
70. Haus, H. A., and W. P. Huang, "Mode coupling in tapered structures," *IEEE J. Lightwave Technol.*, Vol. 7, 729–730, 1989.
71. Cai, Y., T. Mizumoto, and Y. Naito, "Analysis of the coupling characteristics of a tapered coupled waveguide system," *IEEE J. Lightwave Technol.*, Vol. 8, 90–98, 1990.
72. Huang, W. P., and H. A. Haus, "Self-consistent vector coupled-mode theory for tapered optical waveguides," *IEEE J. Lightwave Technol.*, Vol. 8, 922–926, 1990.
73. Huang, W. P., and B. E. Little, "Power exchange in tapered optical couplers," *IEEE J. Quantum Electron.*, Vol. 27, 1932–1938, 1992.

74. Huang, W. P., and S. Lessard, "Wavefront-tilt in nonparallel optical waveguides," *IEEE J. Lightwave Technol.*, Vol. 10, 31322, 1992.
75. Lessard, S., and W. P. Huang, "Assessment of coupled-mode theory for tapered optical coupler," *IEEE J. Lightwave Technol.*, Vol. 11, 405–407, 1993.
76. Chen, Y., "Solutions to full coupled wave equations of nonlinear coupled systems," *IEEE J. Quantum Electron.*, Vol. 25, 2149–2153, 1989.
77. Chuang, S. L., "Application of the strongly coupled-mode theory to integrated optical devices," *IEEE J. Quantum Electron.*, Vol. 23, 499–509, 1987.
78. Donnelly, J. P., H. A. Haus, and N. Whitaker, "Symmetric three-guide optical coupler with nonidentical center and outside guides," *IEEE J. Quantum Electron.*, Vol. 23, 401–406, 1987.
79. Donnelly, J. P., L. A. Molter, and H. A. Haus, "The extinction ratio in optical two-guide coupler $\Delta\beta$ switches," *IEEE J. Quantum Electron.*, Vol. 25, 924–932, 1989.
80. Tomabechi, Y., and K. Matsumura, "Improved analysis for the coupling characteristics of two rectangular dielectric waveguides laid in different layers," *IEEE J. Quantum Electron.*, Vol. 24, 2359–2361, 1988.
81. Huang, H. S., and H. C. Chang, "Analytical expressions for the coupling between two optical fiber core with α-power refractive-index distribution," *IEEE J. Lightwave Technol.*, Vol. 7, 694–702, 1989.
82. Huang, H. S., and H. C. Chang, "Analysis of optical fiber directional coupling based on the HE_{11} modes – Part I: the identical-core," *IEEE J. Lightwave Technol.*, Vol. 8, 823–831, 1990.
83. Marcatili, E. A. J., L. L. Buhl, and R. C. Alferness, "Experimental verification of the improved coupled-mode equations," *Appl. Phys. Lett.*, Vol. 49, 1692–1693, 1986.
84. Peall, R. G., and R. R. A. Syms, "Comparison between strong coupling theory and experiment for three-arm directional couplers in $Ti : LiNbO_3$," *IEEE J. Lightwave Technol.*, Vol. 7, 540–554, 1989.
85. Chen, K., and S. Wang, "Cross-talk problems in optical directional couplers," *Appl. Phys. Lett.*, Vol. 44, 16168, 1984.

86. Haus, H. A.. and N. A. Whitaker, "Elimination of cross talk in optical directional couplers," *Appl. Phys. Lett.*, Vol. 46, 1–3, 1985.
87. Somekh, S., and A. Yariv, "Phase matchable nonlinear optical interactions in periodic thin films," *Appl. Phys. Lett.*, Vol. 21, 140–141, 1972.
88. shank, C. V. C. V. R. L. Fork, R. Yen, R. H. Stolen, and W. J. Tomlinson, *Appl. Phys. Lett.*, Vol. 40, 761–763, 1982.
89. Elachi, "Waves in active and passive periodic structures: a review," *Proc. IEEE.* Vol. 64, 1661698, 1976.
90. Gaylord, T. K., and M. G. Moharam, "Analysis and applications of optical diffraction by gratings," *Proc. IEEE.*, Vol. 73, 894–983, 1985.
91. Yariv, A., M. Nakamura, "Periodic structures for integrated optics," *IEEE J. Quantum Electron.*, Vol. QE-13, 423–348, 1977.
92. Elachi, C., and C. Yeh, "Frequency selective coupler for integrated optics systems," *Opt. Commun.* Vol. 7, 201–203, 1973.
93. Yeh, P., and H. F. Taylor, "Contradirectional frequency-selective couplers for guided-wave optics," *Appl. Opt.*, Vol. 19, 2848–2855, 1980.
94. Syms, R. R. A., "Optical directional coupler with a grating overlay," *Appl. Opt.*, Vol. 24, 717–726, 1985.
95. Marcuse, D., "Directional couplers made of nonidentical asymmetric slabs. Part I: synchronous couplers," *IEEE J. Lightwave Tech.*, Vol. LT-5, 113–118, 1987.
96. Y. Yamamoto, T. Kamiya, and H. Yanai, "Improved coupled mode analysis of corrugated waveguides and lasers," *IEEE J. Quantum Electron.* Vol. QE-14, 245–258, 1978.
97. Hardy, A., "Exact derivation of coupling coefficients in corrugated waveguides with rectangular tooth shape," *IEEE J. Quantum Electron.*, Vol. QE-20, 1132–1139, 1984.
98. Huang, W. P., and H. A. Haus, "Power exchange in grating-assisted couplers," *IEEE J. Lightwave Tech.*, Vol. 7, 920–924, 1989.
99. Grieffel, G. M., Itzkovitch, and Amos Hardy, "Coupled mode formulation for directional couplers with longitudinal perturbation," *IEEE J. Lightwave Tech.*, Vol. 27, 985–994, 1991.
100. Huang, W. P., J. Hong and Z. M. Mao, "An improved coupled-mode formulation for grating-assisted co-directional couplers," *IEEE J. Quantum Electron.*, to be published.

101. Hall, D. G., "Coupled-mode theory for corrugated optical waveguides," *Opt. Lett.*, Vol. 15, 619–621, 1990.
102. Weller-Brophy, and D. G. Hall, "Local normal mode analysis of guided mode interactions with waveguide gratings," *IEEE J. Lightwave Technol.*, Vol. 6, 1069–1082, 1988.
103. Chen, C., and A. W. Snyder, "Grating-assisted couplers," *Opt. Lett.*, Vol. 16, 217–219, 1991.
104. Ogawa, K., W. S. C. Chang, B. L. Sopori, and F. J. Rosenbaum, "A theoretical analysis of etched grating couplers for interated optics," *IEEE J. Quantum Electron.*, Vol. QE-9, 29–42, 1973.
105. Yamamoto, Y., T. Kamiya, and M. Yanai, "Improved coupled mode analysis of corrugated waveguides and lasers," *J. Quantum Electron.*, Vol. QE-14, 245–258, 1978.
106. Cook, J. S., "Tapered velocity couplers," *Bell Sys. Tech. J.*, 807–822, 1955.
107. Fox, A. G., "Wave coupling by warped normal modes," *Bell Sys. Tech. J.*, 823–852, 1955.
108. Louisell, W. H., "Analysis of the single tapered mode coupler," *Bell Sys. Tech. J.*, 853–870, 1955.
109. Matsuhara, M., and A. Watanabe, "Coupling of curved transmission lines, and application to optical direction couplers," *J. Opt. Soc. Am.*, Vol. 65, 163–168, 1975.
110. Alferness, R. C., "Optical directional couplers with weighted coupling," *Appl. Phys. Lett.*, Vol. 35, 260–262, 1979.
111. Abouzahra, M. D., and Lewin, "Coupling of degenerate modes on curved dielectric slab sections and application to directional couplers," *IEEE Trans. MTT.*, Vol. MTT-28, 1091101, 1980.
112. Ramer, O. G., C. Mohr, and J. Pikulski, "Polarization-independent optical switch with multiple sections of $\Delta\beta$ reversal and a Gaussian taper function," *IEEE J. Quantum Electron.*, Vol. QE-18, 1772, 1982.
113. McHenry, M. A., and D. C. Chang, "Coupled-mode theory of two nonparallel dielectric waveguides," *IEEE Trans. MTT.*, Vol. MTT-32, 1469–1475, 1984.
114. Weissman, Z., A. Hardy, and E. Marom, "On the applicability of the coupled mode theory to non-parallel waveguide systems," *Opt. Comm.*, Vol. 71, 341–344, 1989.

115. Snyder, A. W., "Surface mode coupling along a tapered dielectric rod," *IEEE Trans. Antennas Propagation,* Vol. 13, 821–822, 1965.
116. Snyder, A. W., "Coupling of modes on a tapered dielectric cylinder," *IEEE Microwave Theor. Tech.,* Vol. 18, 383–392, 1970.
117. Yasumoto, K., "Coupled mode analysis of two-parallel circular dielectric waveguides using a singular perturbation technique," *IEEE J. Lightwave Technol.,* Vol. 12, 74–81, 1994.